UNIVERSITY OF CAPE COAST

ASSESSMENT OF SEASURFACE TEMPERATURE AFFECTING CORAL BLEACHING IN THE ERITREAN SOUTHERN RED SEA

HERMON GHEBRESLASSIE BELAY

2021

Hermon Ghebreslassie Belay

University of Cape Coast

UNIVERSITY OF CAPE COAST

ASSESSMENT OF BIOPHYSICAL PARAMETERS AFFECTING CORAL BLEACHING IN THE ERITREAN SOUTHERN RED SEA

BY

HERMON GHEBRESLASSIE BELAY

Thesis submitted to the Department of Fisheries and Aquatic Sciences of the School of Biological Studies, College of Agriculture and Natural Sciences, University of Cape Coast, in partial fulfillment of the requirements for the award of Master of Philosophy degree in Integrated Coastal Zone Management

NOVEMBER, 2021

DECLARATION

Candidate's Declaration

I hereby declare that this thesis is the result of my own original research and that no part of it has been presented for another degree in this university or elsewhere.

Candidate's Signature ……. Date ……..

Name: Hermon Ghebreslassie Belay

Supervisor's Signature

We hereby declare that the preparation and presentation of the thesis were supervised in accordance with the guidelines on supervision of thesis laid down by the University of Cape Coast.

Principal Supervisor's Signature…… Date ……

Name: Prof. Frederick Ato Armah

Co-Supervisor's Signature…… Date ……...……

Name: Dr. Isaac Okyere

ABSTRACT

Coral reefs, a spectacular marine ecosystem, have species diversity that significantly exceeds any other marine environment. However, they are among the most heavily degraded and sensitive marine ecosystems. In the literature, there is little information about coral reef distribution and oceanographic factors influencing reef health. To generate preliminary data on the Eritrean southern Red Sea, to serve as a baseline for future coral reef management and monitoring initiatives, two sites from around Massawa, and one around Dahlak Island, Eritrea were selected to collect data on coral reef distribution and bleaching which was used as a benchmark for the data obtained from a satellite. A line intercept transect method was employed to survey the benthic communities. Three imagery classification methods (MLC, Random Forest, and SVM) were employed to assess the distribution of the different benthic habitats. The SVM model had the highest classification accuracy of 74%. The study showed that there was a remarkable decline in live coral cover between the years 2013 and 2020. Results from MANOVA and ANOVA tests illustrate a significant difference in live and dead coral coverage among the three sites. Furthermore, time series analysis on the sea surface temperature (SST) and sea surface temperature anomaly (SSTA) data indicated a significant increase in sea surface temperature around the southern red sea, and it is predicted that this trend will continue in the next 10 years. Results from this study indicate that the reefs around Massawa show a rapid decline in live coral cover, hence, the study calls for the instigation of management plans towards the conservation of coral reefs in the region.

ACKNOWLEDGEMENTS

My heartfelt thanks go to the ACECoR/UCC Fisheries and Center for Coastal Management for providing the financial support required to conduct this research. I would also like to thank my supervisors, Prof Fredrick Ato Armah and Dr. Isaac Okyere of the Department of Fisheries and Aquatic Sciences (DFAS), for their professional and scientific guidance, advice, encouragement, and goodwill in guiding this work. I am grateful to Mr. Richard Adade, CCM Research Fellow. Ms. Esther Acheampong, a postgraduate student at DFAS, deserves special recognition for her selfless assistance in structuring and editing aspects of the work. I also want to thank Mr. Zayid Gebrezgiabiher, a research fellow at the Ministry of Marine Resources, for his selfless assistance during data collection in the field. I am also grateful to the DFAS and CCM staff and postgraduate students for their enormous contribution to the success of this work through their participation in seminars to provide vital inputs. Last but not least, I owe my most profound appreciation to my beloved parents, for their extraordinary patience and my husband Dr. Huruy D Asfha for being by my side and always giving me the strength and astuteness to be sincere in my work, for setting high moral standards and supporting me through hard work.

DEDICATION

To my father Mr. Ghebreslassie Belay Demer.

TABLE OF CONTENTS

LIST OF TABLES

LIST OF FIGURES

ACRONYMS

Chl-a	Chlorophyll-a
CRW	Coral Reef Watch
GAIW	Gulf of Aden Intermediate Water
GASW	Gulf of Aden Surface Water
GIS	Geographical Information System
MODIS	Moderate Resolution Imaging Spectroradiometer
RSOW	Red Sea Outflow Water
SST	Sea Surface Temperature
SVM	Support Vector Machines

CHAPTER ONE

INTRODUCTION

Background to the study

Coral reefs are one of the most diverse and remarkably useful marine ecosystems on earth. They are valuable socio-economic resources as they are high in biodiversity and serve as fishing grounds for commercial fisheries, providing consumers with protein and ornamental fishes (Baswapoor & Irfan, 2018). They attract many tourists; thus, generating significant contributions to the national income of several nations, especially developing countries. (Wolanski., et al 2003). They also provide natural protection against coastal erosion and storm damage (Hoegh-Guldberg et al., 2019). Humans, however, have been disrupting the reefs since they began interacting with them. Over the last 40 years, anthropogenic effects like pollution, overfishing, and climate change have hastened their global deterioration (Spalding & Brown, 2015).

Targeted interventions may counteract this destruction with the help of tools such as the creation of marine protected areas and reef restoration projects. However, its effectiveness rests massively on our understanding of the location and status of the earth's reefs. (Purkis et al., 2019).

Natural recovery of reefs may be improbable, and the resolution may have to be artificial rehabilitation. Many organizations undertake the rehabilitation of coral reefs, planting corals each year (Ladd et al., 2018). The success of this practice is impeded by high spatial variability in the state of the reef restoration. The high spatial variability in reef conditions, on the other hand, limits our understanding of where restoration is required. In providing a solution to this, Shawna & Gregory (2019) stated that “Remote sensing can be

helpful to access a global map of the condition and distribution of reefs at high spatial resolution and temporal frequency, enhancing accuracy in determining the regional impacts of climate change on reefs. From 2005 to 2007, Eritrea's Coastal Marine Island Biodiversity (ECMIB), a group dedicated to Island biodiversity and conservation projects embarked on an expedition in Eritrea. The primary goals of the Red Sea Reef Expedition were to map and characterize coral reef ecosystems, identify their status and major threats, examine factors affecting their resilience, and promote local and regional conservation efforts through data sharing, outreach, and education (Rasul & Stewart, 2015).

Coral bleaching due to the increase in sea surface temperature (SST) remains danger to coral reefs. Tropical regions saw extremely high Sea Surface Temperatures between 1997 and 1998, resulting in the "largest bleaching episode yet recorded" (Wilkinson et al., 1999). Global warming was considered the underpinning factor to this occurrence (Reaser et al., 2000). Global warming is expected to cause more incessant and intense coral bleaching in the future (Spalding & Brown, 2015).

Statement of the Problem

The Red Sea is known as a place with vast endemic biodiversity (DiBattista et al., 2016). Besides the variety and history of research work in the region, knowledge of the Red Sea coral reef ecology lags behind that of other large coral reef ecosystems. On average, research conducted in the Red Sea makes up only one-fifth of works done on the Great Barrier Reef and around one-eighth of those from the Caribbean (Berumen et al., 2013). Furthermore, over 50% of the studies reported on the Red Sea focus on the

Gulf of Aqaba, a narrow region in the far northern Red Sea that occupies less than 2 percent of the Red Sea territory (Berumen et al., 2013).

Coral reef ecosystem degradation has accelerated over the last three decades as a result of increased anthropogenic disturbances and their interactions with natural stressors. These stressors are thought to cause coral bleaching, resulting in coral cover loss. Unfortunately, little is known about the prevalence, and distribution of coral bleaching in the Red Sea at the moment (Mona et al., 2019).

The global reduction in coral coverage is a significant concern as a result of global warming and associated overfishing, coral bleaching, coastal pollution, and tourism-related coral breakage. Particularly temperature-induced bleaching of corals is an alarming threat to coral reef ecosystem biodiversity (Muller-Parker et al., 2015). Perhaps, the lack of a suitable methodological approach to assessing the location of the corals and the inability to cover large areas at the same time explains the limited knowledge available on corals. According to Mason et al. (2020), remote sensing plays an important role in predicting coral bleaching by providing information on sea surface temperature, cloud cover, wind, and other climate parameters. Yet, only a few publications on mapping and monitoring the beginning of coral bleaching at various spatial scales have been published. Remote sensing, by mapping and monitoring reef ecosystems, assists stakeholders in understanding the phenomenon of coral bleaching forecasts for estimates of when and where bleaching will occur.

Monitoring activities are critical for alerting scientists and conservationists about the state of coral reefs worldwide, and detecting

changes in habitat quality over time (Lin, 2021). As fragile ecosystems, detecting temporal coverage variations in coral reefs will ensure their protection, and the establishment of adequate management efforts to be modified to better address the specific threats posed to these fragile ecosystems (Beenaerts & Berghe, 2005).

Major reef domains have recorded massive coral mortality in reef ecosystems since the 1870s. There has been an increment in reported disruptions in coral reef ecosystems although in the past few years the focus was on the magnitude and frequency of coral bleaching. Coral reef bleaching events surveyed from 1979 to 1990, revealed that out of 105 coral mortality cases, 60 of them were due to coral bleaching. This figure is alarming, considering that, only 3 bleaching events were reported 103 years before 1979, where total reported coral mortality cases were 63 (Glynn, 1996).

Objectives of the Study

This study seeks to generate baseline information and preliminary data from the southern Red Sea which can be used as a baseline for future coral reef management and monitoring schemes. Thus, the information provided would serve as a reference point for coastal resource managers and tourism directors in Africa and Middle Eastern countries regarding the status and environmental trends of the species.

The specific objectives were to:

I. To design and validate habitat mapping of coral reefs and coral reef change detection around the Massawa region.

II. To determine and model the effect of temperature, and chlorophyll-a concentration on coral reefs around the Massawa region.

III. To determine the efficiency of Degree Heat Week (DHW) as a coral bleaching index in the central region using bleaching occurrence/ non-occurrence under temperature fluctuations.

The following hypotheses were therefore tested based on the set objectives:

H_0: Yearly average sea surface temperature in the three sites under consideration is equal.

H_1: The average yearly temperature in the three sites is different.

H_0: Yearly average sea surface temperature anomaly in the three sites is the same.

H_1: The yearly average sea surface temperature anomaly is not the same.

H_0: Sea surface temperature is increasing over the years.

H_1: Sea surface temperature shows no significant increment over the years.

H_0: Live coral coverage is decreasing over the years.

H_1: No significant decrement in live coral coverage exists.

Significance of the Study

The Theory of Change in the zero drafts (Annex I-II; Paras C. 5-8) highlights that "combined action on the state of nature, economic systems, and social values are necessary to achieve sustainability." In the Global Biodiversity Framework (GBF), it is stipulated that "while the timeline of Agenda 2030 corresponds to the needed 2030 Mission for the GBF, it also provides language to identify the 'safe corridor' or trajectory towards achieving the 2050 biodiversity vision, and a broader vision combining nature, economy, and society that countries will need to identify after 2030." It is with this

agenda that the need for mapping and understanding of coral ecosystems such as the coral reefs of the Southern Red Sea rests. With the awareness created from this research, efforts on coral reef conservation would increase, allowing for management efforts to be modified to counter the specific threats posed to these fragile ecosystems (Beenaerts & Berghe, 2005).

The research output will be a basic study of the changes in sea surface temperature in time along the Eritrean Red Sea which will be necessary for filling a knowledge gap concerning coral reef decline. Yearly and seasonal SST and Chl-a studies permit the ability to investigate the spatial and temporal patterns of the marine ecosystem and can provide important insights into seasonal and temporal variation of fisheries productivity in the Eritrean Red Sea.

The total fish biomass is a function of the available healthy coral community. Highly productive fisheries areas are usually associated with a healthy ecosystem (Solanki et al., 2005). As a result, the findings of this study can aid in determining the number and biodiversity of other marine creatures. This, in turn, has an impact on fisheries, which is a vital source of protein for many of the region's poorest residents.

This research work intends to build on the knowledge base of biodiversity in the Sothern Red Sea by serving as a baseline for establishing management and conservation measures. It also seeks to raise awareness of coral bleaching and the need to enact regulations against coral bleaching. The study area was chosen because it is a hotspot of tourism and recreation and the largest port in Eritrea is located there. It is suspected that the economic

activities occurring within the region have detrimental effects on its diverse coral reef ecosystem.

Delimitation of the Study

There are several Islands in Eritrea. The islands chosen for conducting this research were selected based on two main criteria: first, they are areas of high marine biodiversity that are affected by increasing sea surface temperature. Secondly, they are known as sites of high anthropogenic activities. This is because, unlike other Islands in the region, public use of those islands is not prohibited.

Limitation of the Study

The unavailability of data on chlorophyll-a in the study areas and Eritrea in general prior to the year 2013 restricted the study on chlorophyll-a to 2013. Thus, the correlation of temperature to chlorophyll-a could not be established until 2013 due to missing data.

Organization of the study

This thesis is organized into six chapters. Chapter one discusses the concept of the study and provides the context and definition of the investigation's problem, purpose, objectives, and importance. The second chapter examines the literature relevant to the study. An in-depth assessment of the literature on global coral reef threats is presented.

The research methodologies are outlined in Chapter Three, with diagrams when applicable. The study areas are well-described, and the statistical methods and programs utilized to analyze the data acquired are discussed. The results and comments are presented in Chapters Four and Five, respectively. In Chapter Four, the research findings are presented in the form

of tables, graphs, charts, and maps with summaries. Chapter five discusses a detailed examination of data and inferences shown in the form of a conversation organized around the study's primary themes. Chapter six contains the conclusions and recommendations. A list of references and appendices is also included in this thesis.

Chapter Summary

This chapter presents the study's broad reasoning and the various stakeholders' justifications and benefits from coastal management and keywords and abbreviations explained to readers.

CHAPTER TWO

LITERATURE REVIEW

The International Hydrographic Organization described the Red Sea as a semienclosed humid basin circumscribed by the Arabian Peninsula in the east and northeastern Africa. According to Behairy et al. (1991), the tropical and sub-tropical conditions of the Red Sea experience deficiency of rainfall (averaging 6 cm per year) with vaporization levels reaching 205 cm per year.

Throughout the Red Sea basin, the apparent water temperatures of the Red Sea oscillate between 21ºC and 28ºC in the north and 26ºC and 32°C in the south (Nandkeolyar et al., 2013). Furthermore, the comparative moisture throughout the Red Sea basin differs from an extreme of 68% during summer to at least 50% during winter, and daylight clamminess levels are considerably greater than at night. The airstream is categorized by autumn and local disparities in both direction and speed, with average rates mostly accumulated toward the north (Patzert, 1974). According to Rao & Behairy (1986), the predominant wind speed that varies from 7 to 12 km per hour is primarily north to northwest, with intermittent southerly winds in the winter.

Research proves that the utmost substantial confirmation of marine rifting acknowledged streaky hypnotic irregularities along the southern Red Sea axis (Phillips, 1970; Searle & Ross, 1975; Cochran, 1983). Researchers did not condone the phase of the glitches once equated to global magnetostratigraphic, but they did conclude that the striping epitomizes the autograph of factual marine spreading. The southern Red Sea is currently described as a marine fissure. Hence there is explicit agreement that the

northerly point of the crack, the Gulf of Suez, is mainly continental in eccentric (Jarrige et al., 1986; Girdler & Southren, 1987).

Prefatory to coral reefs

Despite being highly valuable and diverse, coral reefs are one of the most endangered ecological units on the earth (Plaisance, 2011). Environmental variation, coastline enlargement and tourism, caustic fishing, and other human accomplishments threaten their actual survival. Currently analyzing the degree of destruction, over a third of the biosphere's coral reefs may be shattered within our generation, which means that there could be overwhelming harm to biotic diversity, coastline fortification, income, food, and research (Ramesh et al., 2020). According to Wilkinson (2008), the variety, rate, and measure of anthropogenic influences on coral reefs are accumulated to the degree that reefs are generally endangered. Effluents, pollutants, and sediments from land-based activities has been the significant trigger of enormous and fast-tracking falls in the profusion of coral reef species (Pandolfi et al., 2003).

Experts of aquatic biology on coral reefs use several different classes of statistics, from manifold time eras to study the past topical history and present state of reef ecosystems to supply a common standard for collaborative ecosystem and coral development degrees. Numerous mass extinctions related to coral reefs have been experienced over geological time. Reefs have subsisted fluctuating sea echelons, elevating landmasses, phases of extensive warming and recurred ice ages, and repeated short-term non-human catastrophes such as storms and hurricanes. Coral reefs have displayed the significant capability to acclimate and subsist over geological years.

In literatures, it is outlined that the coral reef system has experienced methodical collapse preceding contemporary environmental research in the last three or four decades. This is in line with Gillespie (2020), who indicated that no reef can be measured as "pristine" and that no stock occurs by which to associate the degree of these variations. Despite the palaeoecological restoration of Caribbean Sea reefs, a recent study has focused on the regional breakdown of coral communities, which is unusual for the Holocene (Greer et al., 2002) and Pleistocene, (Pandolfi & Jackson, 2006).

Characteristics and morphology of coral reefs

Bellwood et al. (2004) stated that coral reefs are well-distinct as three-dimensional superficial water configurations subjugated by Scleractinia corals. According to the Alliance (2003), coral reefs are colossal limestone configurations that offer food and shelter for marine life. Hard corals are accountable for much of the reef's solid, limestone (calcium carbonate) structure. Approximately coral reefs are so massive that they can be perceived from outer space because they were assembled over hundreds, if not thousands of years. Comprehensively, the limestone structure of coral reefs harbors a diverse collection of plants and animals. Calcareous algae, which have limestone in their tissues, help construct the reef while worms, grazing fish, urchins, and boring sponges break it down.

Environmental conditions must always be favorable to help establish a healthy coral reef due to their high sensitivity. According to Alliance (2006), reef-constructing corals cannot persist in sunlight deprivation since zooxanthellae, their interdependent algae, need sunshine for photosynthesis. Below 45 m (150 ft), the mainstream of zooxanthellae reef-construction corals

do not propagate. Constricted high temperatures varying from about 16 to 29°C support corals' survival and growth, which can be attributed to why corals flourish in the furnace waters of the tropics.

Nevertheless, nutrients required by corals are found in food and are water dissolvable. Although, several nutrients can distraught the usual equilibrium of life on the reef, resulting in situations that enable other fast-developing species such as marine plants and sponges. Preferably, corals thrive well in clear water with squat echelons of residues (tiny particles of earth, rock, and sand). Residues could conceal corals, hindering out required sunshine and destroying them. Glynn (1993) stated that corals are aquatic animals modified to animate in seawater with about 35 parts per thousand salinity. Corals cannot thrive in regions that are hypersaline or not saline enough. Corals require a firm substrate to fasten and do not effectively settle on unfastened substrates such as rubble or sand. The unstable bottom promotes the destruction of young coral colonies by wave action and storms.

Globally, coral reefs shield approximately 284,300 square kilometers (Schgal, 2006). Representatively, this zone is below 0.1% of the biosphere's oceans and not more than 1.2% of the interior shelf area. All over the world, coral reefs are found surrounded by the tropics (amid 30^{o} north and 30^{o} south of the equator). Gynn (1993) reported that coral reefs can be in three extensive sections: the Caribbean and Atlantic, the Indian Ocean and the Red Sea, the Pacific, and Southeast Asia. The Indo-Pacific, which stretches from the Red Sea to the Central Pacific, is home to the majority of coral reefs. The highest species diversity occurs in this area among the overall reefs. Approximately

80% of the ecosphere's coral reefs are in the Caribbean and Atlantic, and species variety is very few in these areas (Bellwood & Wainwright, 2002).

Generally, taxonomists have categorized coral reefs into 5 focal groups: fringing, barrier, atolls, bank or platform, and patch reefs (Alliance, 2006). Fringing reefs are mostly found on opposite sides of islands and continents and are divided from the coast by narrow, superficial lagoons. Frequently, they are analogous to the coast and, at their narrowest point, can extend to the water's surface. On the other hand, barrier reefs grow comparable to the shoreline but are divided by deep, vast lagoons. They easily extend the water's superficial, establishing a "barrier" to triangulation at their shallowest point. The famous Great Barrier Reef in Australia is the most significant in the world (Wilkinson, 2008). Positioned in the center of the sea are atolls characterized by rings of coral that create protected lagoons.

Open Ocean reefs like banks or platform reefs have artless configurations with numerous diverse roots, however no particular connection to the shoreline. Records show that most of these reefs possess an area wide open to wind and a protected side where lagoons and small reef patches can be located. Descriptively, more significant and marginally water-logged reefs of this type are also known as shoals, whereas patch reefs are small areas of reef that are characterized by their existence in shallow waters and lagoons (Polovina,1984).

Coral reefs are very distinctive, and divergent from one another. However, they have related patterns or zones that can be recognized on supreme reefs, grounded on profundity, ecological factors, reef configuration, and species composition. Harborne et al. (2012) described that the intertidal

zone, reef flat, reef back, reef crest, or algal ridge, and fore reef or reef front are said to be the regions and associated bionetworks located in several coral reefs all over the biosphere.

The intertidal zone comprises coasts, mangroves, ponds, and zones where freshwater meets saltwater and is sometimes described as where the land meets the ocean. Seashores are imperative for coral reefs, as they sift out overflow and sediments from the land. The natural breakdown of coral fragments results in an abundance of sand on beaches. Extremely adapted plants such as mangroves can succeed in intertidal waters and are also enormously significant for coral reefs, filtering mud and sediments from the land, and as interim nurseries for juvenile reef species. According to Burkepile & Hay (2008), reefs near complete mangroves can have up to 26 times more fish than reefs further from mangroves.

Usually, corals are either categorized as hard or soft. Descriptively, Scleractinia corals (hard) are defined as the principal reef-building animals and are liable for the limestone groundwork of tropical coral reefs whereas soft corals lack the reef-building ability and their counterparts' gorgonians (sea fans and sea whips) forming an essential part of the coral reef ecosystem, stirring in most reef habitats, and exhibiting a glittering collection of colors and shapes (Dewi et al., 1996).

Individually, a stiff coral polyp matures within its hard cup or "calyx," where it lays down a limestone frame, and when the polyp perishes, its limestone skeleton is left behind and is used as the template for a different polyp. The framework of the reef is created when layer upon layer builds up over time, and the superficial of the structure forms a shrill layer of living

coral animals. Presently researchers approximate that there are around 794 classes of reef-building corals all over the biosphere. Classifying coral classes can be remarkably challenging even for researchers. Most model technique for the classification of corals is based on their diverse shapes. Balasubramanian (2016) acknowledged that coral development forms can be categorized into ten, namely branching, elkhorn, digitate, encrusting, table, foliose, massive, submassive, mushroom and, flower/cup that look like flowers, or like egg cups that have been compressed, elongated or twisted. Though development configurations are predominantly species-specific, the particular similar coral can seem precisely diverse from one place to the next, varying its shape, color, and size to suit its atmosphere. Mainly, they develop into more complex forms, such as elusive branching patterns in more sheltered areas.

Corals cannot feed on their own, and hence they need their symbiotic companions. Zooxanthellae is a microscopic single-celled alga found within the tissues of complex coral polyps (Polovina, 1984). Quite a few millions of these algae dwell in just one square inch of coral and result in the brownish-green description of corals. Zooxanthellae and corals have an interdependent relationship that both benefit from each other (Leigh, 2010). This association is compound and not yet fully comprehended. It is believed that the algae provide the coral with calcium carbonate, energy, and nourishment, whereas the coral polyps provide zooxanthellae with shelter and nutrient recycling. Corals described as hard are enormously dependent on zooxanthellae and usually cannot persist without it unless they can obtain sufficient nourishment by netting plankton from the water column (Jeffrey & Haxo, 1968).

According to Bellwood & Wainwright (2002), stress is causing the coral polyp to remove its symbiont algae; hence, looks white (bleached). Although utmost hard corals appear to be sensitive without symbiotic algae for minor phases of time, they frequently perish over the long term throughout extreme or widespread bleaching event stresses.

Bleaching of coral reefs

According to Glynn (1993), the damage of endosymbiotic algae (zooxanthellae) and/ or a decrease in the photosynthetic colorant concentrations within the zooxanthellae that many hostile ecological circumstances can instigate is described as coral bleaching.

Despite their abundance, coral reefs are one of the most fragile oceanic bionetworks, according to Hoegh-Guldberg (1999). Coral bleaching has caused an unnatural reef layout as a result of the warm weather. Corals and other zooxanthellae invertebrates lose the acute stability that allows them to maintain their symbiotic relationship with zooxanthellae when they are stressed (Reaser et al., 2000). This results in the ejection of zooxanthellae and/or a decrease in photosynthetic colorant absorption within the zooxanthellae (Booth & Beretta, 2002). The resultant change in color as a result of stress in corals and other invertebrate hordes comprises compact salinity, decline or upsurge in light, impulsive and prolonged variation in temperature, contamination from heavy metals and agricultural chemicals and biological elements like bacteria (Hoegh-Guldberg, 1999).

Nevertheless, utmost bulk coral bleaching happenings are instigated by ecological factors, for example, irradiance or an increase in temperature (Baker et al., 2008). As stated by Glynn (1996), research shows a mutual

rapport between eminent sea temperatures and mass coral bleaching happenings. Generally, corals that are bleached mislay 60-90% of their zooxanthellae entities. Furthermore, outstanding zooxanthellae might lose up to 80% of their photosynthetic tints (Glynn, 1996). The coral becomes white (bleached) after these symbiotic dinoflagellates are ejected (Goreau & Macfarlane, 1990). The level of photosynthetic efficiency declines, according to Coles & Jokiel (1978), and this is the main source of energy for calcification (Muscatine, 1990). The coral's capacity to progress and compete for space with other species, such as macroalgae, will be harmed (Hoegh-Guldberg, 1999).

Since 1979, there have been six major bleaching events, all of which have been triggered by rising seawater temperatures in conjunction with global climatic change and El Niño /La Niña occurrences, as well as the likely synergistic impacts of increased UV and visible light (Hoegh-Guldberg et al. 2005). According to McPhaden (1999), the El Niño Southern Oscillation (ENSO) was unique, with higher sea surface temperature (SST) globally in 1997/1998, causing up to 90% coral impermanence in some zones (Wilkinson, 2000). As stated by Hoegh-Guldberg (1999), the rate and rigorousness of bleaching occurrences are expected to upsurge in the coming years. Therefore, it can be deduced that elevated CO_2 levels and SST can lead to an augmented rate and rigorousness of the bleaching process. Higher concentrations of CO_2 may constitute reduced frequencies of reef calcification and dissolution of coral skeletons.

Furthermore, effects on supplementary biological processes in coral reefs and other reef-building species are probable. According to Cantin &

Lough (2014), researchers have detected an upsurge in the world's rate, concentration, and degree of bleaching occurrences since the 1980s. This results from the increase in ocean superficial temperature due to global warming, coupled with the fortification of the El Niño occurrence.

In 2010, an extreme El Niño occurrence triggered coral bleaching, distressing all reefs through the biosphere with more significant growth and death in some areas like South-East Asia (Hedberg et al., 2015). The bleaching incident in the years 2014 to 2017 was unique and of extraordinary degree. In contrast, the third bleaching chapter commenced in June 2014 in the western Pacific, then extended to the Marshall Islands and the Florida Keys. In 2015, the sensation stretched to the Indian Ocean, the South Pacific, the central and eastern zones of the steamy Pacific, and the Caribbean. By the end of 2015, when El Niño was attaining its peak, 32% of the biosphere's reefs had been uncovered to a temperature glitch of +4°C, instigating coral mortality over more than 12,000 km² (Ampou, 2017).

Generally, coral reefs are defined as frameworks of the world's aquatic biodiversity and are habitats to more than a third of all oceanic creatures, comprising 4,000 species of fish. Nevertheless, when reef-building coral experiences bleaching and dies, an entire biodiversity pool is threatened. After the 2016 heat wave, researchers recounted a reduction in the large quantity and assortment of herbivorous fish species (Hughes et al., 2019), like the damselfish in regions of the Great Barrier Reef (Hughes et al., 2018). The deterioration in herbivorous populations is supplementary distressing. They play an efficient central role in reef improvement, persistence, and resilience

by overriding the filamentous algae that take possession of coral (Hughes et al., 2019).

Red Sea oceanography

The Eritrean shoreline is artistic, resource-rich, and home to a wide variety of wildlife (Sebhatu, 2019). Because the area is lightly populated and the fishery sector is not industrialized, there are few anthropogenic stresses. Nonetheless, climate change has a negative influence on the coastal ecosystem, as seen by coral bleaching and rising sea levels.

The Red Sea approximately accounts for merely 0.12% of the overall water, but it is home to 6.2% of worldwide coral reefs (Wilkinson, 2008). Globally, the Red Sea is the primary hotspot for the coral reef ecosystem. It is considered part of the Indo-Pacific area and comprises the greatest variety of reef species behind the Southeast Asian 'coral triangle' (DeVantier et al., 2000).

Climate change and anthropogenic compressions have a negative impact on coral reef ecosystems and, as a result, on the safety of societies that rely on bionetwork resources for survival. Instigators of coral reef deterioration comprise sedimentation, vicious fishing, the intense advance of the tourism industry, land recuperation for coastal improvement, an extreme surfeit of nutrient-burdened rivers, and climate variation (Goldberg & Wilkinson, 2004).

Frequently Coral Reefs are found alongside the 1,350 km of the coast of Eritrea, approximately 18 % of the Red Sea, and about supreme of its 350 islands, stirring as blotches in a comparatively primeval state. Between 1993 and 2006, several assessments and treks were piloted to review Eritrean coral

reefs' condition and passed recommendations for better management mechanisms. Outcomes of prior studies designate an increased miscellany of coral and fish in various regions of the coastline and the islands (De Grissac & Negussie, 2007).

The coral reef ecosystems in the Eritrean Red Sea's central section support a large number of fish and invertebrates that are threatened by artisanal fishing (Tesfamichael, 2016). Similarly, the reefs are household to thousands of fish species comprising numerous widespread species (Zekeria, 2003). Generally, fishing compression on coral reefs is comparatively stumpy, as Eritrea's scorching and arid central littoral regions are not compactly occupied. Conversely, Tsehaye (2007) noted that most zones recurrently invaded by fishers had displayed indigenous diminution and decline. In recent times nevertheless, the expansion of coastal zone is increasing, and the coercions on coral reef well-being are rising (Tesfamichael, 2016). According to Kotb et al. (2008), the coral reefs in the Red Sea South are focused on intermittent bleaching due to increased water temperature throughout the summer months.

During the summer months, specifically August and September, the coral reefs of the central section of the Eritrean Red Sea coast are imperiled to increased temperature. At the end of the summer, when the sea surface temperature exceeds 33 degrees, coral bleaching is common in the Eritrean Red Sea's central region. The Eritrean Red Sea reefs writhed in 1998 due to severe coral bleaching, and the majority of recovery cryptograms were found in the central and northern Eritrean Red Sea. According to Kotb et al. (2008),

in 2007, life-threatening stumpy tides resulted in coral bleaching and transience.

Physical process

Generally, the Eritrean Red Sea area is parched, and rainfall is limited, with yearly middling alternating 1 – 180 mm (Edwards, 1987). According to Morcos (1970), there is vaporization with an almanac average of 2 m. Chaidez (2017) noted that the sea surface temperatures in the south section of the Red Sea to a high of of 33^{o}C. Furthermore, a different feature of the Eritrean Red Sea is the elevation of its salinity which is approximated at around 35 PSU at the surface.

Studies reveal that the high salinity level of the Red Sea is based on the amalgamation of its geographical olden times and the dry and hot surroundings. However, initially, the Eritrean Red Sea depression was swamped with Mediterranean water and owing to increased evaporation, it became more saline. Throughout the icy history, the Eritrean Red Sea was a sequestered salty stream with salinity more significant than the current by a rate of 10 (Goudie & Middleton, 2006).

Biochemical process

The Eritrean Red Sea's middle section is sparsely populated, owing to a lack of nutrient-rich global overflow. There is also no exchange of nutrient-rich bottom-water to the surface, where photosynthesis takes place. A constant thermocline prevents water from mixing perpendicularly because the temperature underneath water is always lower than the warm surface temperature.

The flow of nutrient-rich water from the Indian Ocean, the primary nutrient contributor, and the re-deferment of nutrients from the lowermost deposits by tempestuous fraternization from its wide-ranging and superficial shelf area all contribute to the southern part of the Eritrean Red Sea being more prolific than the northern part. The shallow water of the Eritrean Red Sea is also prolific and chains several subjugated fish populations.

It is postulated that the tremendous and comparatively steady temperature of the Eritrean Red Sea is advantageous for developing coral reefs (Vine, 2019). Naturally, coral reefs have a self-maintained nutrient sequence and have increased efficiency, remarkably like a sanctuary in a desert, and are said to entice fisheries, mostly small-scale artisanal, and sightseers. Froese and Pauly (2011) reported that the central region of the Eritrean Red Sea has precisely great variety, more than 1200 species of fish, and an extraordinary notch of endemism categorize this. The percentage of Eritrean Red Sea endemic fishes range from 10% to 17% (Ormond & Edwards, 1987); the country's semi-sealed vegetation and unique biological conditions contribute to this high number. Because the middle section of the Eritrean Red Sea has extremely low nutrient input, animals that can survive in their environment have a good chance of being overlooked because there are fewer competitors. It's a blue-green alga (cyanobacterium) that nitrate-depletes soils by fitting gaseous nitrogen liquefied in water. The strings of cyanobacterium drift to the sea surface in calm seas, forming a moderately reddish layer that may be the source of the term Red Sea.

Remote sensing-based studies on coral reefs

Globally, research reveals that coral reefs are in the state deteriorating (Bellwood et al., 2004). According to Burke et al. 2011, as of 2011, 19% of reefs had gone extinct, and 75% were endangered. This deterioration results from the unique collective properties of natural and anthropogenic extortions functioning at regional and worldwide levels (Burke et al., 2011). In the Eritrean Red sea's central region, human actions such as coastline improvement, manipulation and disparaging fishing observation, contamination, and runoff have prompted coral reef decline (Burke et al., 2011; Mora, 2011).

Through global warming and oceanic acidification, increasing environmental carbon dioxide has subsidized the dilapidation of these bionetworks and can intensify regional stressors (Baker et al., 2008). There is cumulative responsiveness of the degree of coercions fronting coral reef bio networks (Burke et al., 2011). Intensive care activities have become crucial for assessing the impact of the incident on reefs and tracking future recovery or degradation. Several coral reef-checking curriculums based on on-the-ground investigations have been developed around the world to assess the importance of coral reefs.

The National Oceanic and Atmospheric Administration (NOAA) discovered unusually high SST in the western Coral Sea, about halfway down Australia's Great Barrier Reef (GBR). According to Liu (2003), during the most significant GBR coral bleaching event in 2002, the NOAA’s National Environmental Satellite, Data, and Information Service (NESDIS) supplied satellite data summary as a measure of the Australian Institute of Marine

Science's (AIMS) and the Great Barrier Reef Marine Park Authority's (GMRMPA) fragmentary coral reef health collaboration. The statistics substantiated the significance to AIMS and GBRMPA as they examined and evaluated the advancement of SST during the Australia summertime, allowing them to keep participants, the general public, and all concerned parties informed and up to date. SST coral bleaching "HotSpot" irregularity and "Degree Heating Week" (DHW) graphs are two of the most important coral bleaching products established by NOAA's Coral Reef Watch (CRW) satellite monitoring and forecast component. Preeminent sea surface temperature has been impelled as the prevailing cause of coral bleaching (Hoegh-Guldberg, 1999) and is now measured as the foremost instigator of worldwide reef deprivation (Hughes et al., 2017b).

Biophysical parameters affecting coral reefs

Globally, coral reef bionetworks fluctuate to different managements, obsessed by an amalgamation of human influence, biotic practices, and abiotic conditions (Hughes et al. 2010). Above the sudden variations in ecosystem function and configuration (Hughes et al., 2010), ever-lasting regime changes may bring hefty costs to society through the forfeiture of bionetwork services related to a specific system (Hicks & Cinner, 2014). Coral reef managers face serious challenges (Graham & Nash, 2013), ever since detrimental retrogressive regimes can be challenging and expensive due to strong fortifying reaction contrivances. Variations in fish groups have also been emphasized, either as a teamster of benthic regime movement (Hughes et al., 2007) or their undeviating significance (Chong-Seng et al., 2012).

Managing coral reefs efficiently demands a precise and mostly context-specific comprehending of how several factors conglomerate to maintain or destabilize various regimes. Specifically, discriminating the comparative effect of anthropogenic against biophysical factors is essential to escalating how environmental situations might include perimeter or favor variable management options. Differences in biophysical factors, like waves, wind, and productivity, set normal limits on ecosystem situation even when there is no local human effect (Heenan et al., 2016).

Temperature

The coral reefs in the Eritrean Red Sea's central region are the most diverse and vulnerable bionetwork. The Eritrean Red Sea climate variation and acidification are projected to cause bleaching to approximately 90% of corals by 2060 if contemporary radiations linger (Van Hooindink et al. 2014). Coral bleaching happens when ecological factors disturb the symbiosis, resulting in the removal of its Zooxanthellae from the coral host.

Increasingly, as variations in ecological dynamics stance a contest to their sustained survival, corals can occasionally take careful or adaptive schedules to guarantee their survival. Research has shown that corals can recuperate swiftly, succeeding a stagy deterioration, and repossessions of coral cover have been recognized at numerous locations all over the biosphere (Halford et al., 2004). Corals resist heat stress via a number of contrivances, including obtaining thermally resilient symbionts, amassed physiological contrivances by generating oxidative enzymes, or producing photoprotective composites (Fautin & Buddemeir, 1993). There are numerous biochemical methods of defining coral health and merely counting zooxanthellae density is

a well-known method to screen the health of corals (Solayan, 2016). However, there has been some research observing coral health and its relationship to augmented temperature. It is imperative to recognize corals in the central region of Eritrea that are vulnerable to macroclimate variation and distinguish others from those that are further lenient to augmented temperatures.

Seemly, temperatures can upsurge the change in calcification (Jacques et al. 1983). Generally, the sea temperature correlates with light magnitude, upsurge, and phases of calm water and subsequently distresses coral persistence. Nevertheless, when water temperatures and light intensity surpass standard arrays, coral bleaching can transpire (Chavanich et al., 2012).

The southern part of the Red Sea is considered by strong periodic dissimilarity in ecological circumstances, determined by the Eritrean monsoon scheme. Blistering period temperatures are complex than documented in most other steamy regions, commonly surpassing 34℃ on narrow reef flats (Edwards 1987; Afeworki 2003; Zekeria 2003; Ateweberhan 2004).

Chlorophyll-a

According to recent studies, every phototroph also has pigment and fluorescence attributable to the manifestation of chlorophylls and other photosynthetic colorants. Specially in corals, the phototrophs are the endosymbiotic dinoflagellates Symbiodinium. Every coral species quays explicit clades of Symbiodinium with varied chattels (Lajeunesse et al., 2018). Naturally, there are several chlorophyll referends, each with exclusive phantom physiognomies. Even though the comparative confirmation of Chls in corals is triggered by the surroundings, the two-utmost noticeable chlorophylls existing in the recognized clades of zooxanthellae symbionts are

chlorophyll a (Chl-a) and chlorophyll c2, with Chl-a being extra abundant in supreme coral species (Van Duyl et al., 2002).

Temperature and salinity

The existence of colder waters, which are presumably rich in nutrients, and high Chl-a levels can be explored using SST variability (Raitsos et al., 2015). An essential application of SST sensing is identifying upwelling sites where rising cold water delivers nutrients to the surface, embracing phytoplankton and zooplankton to grow and attract large concentrations of fish.

Air temperature and SST in the Red Sea are highest in the south and decline from south to north, reaching their lowest point in the Gulf of Suez. As shown in Figure 1, the surface SST varies from 26ºC in the north to 33ºC in the south. Due to the influx of cooler water from the Gulf of Aden, the SST along the Strait of Bab-al-Mandeb in the southernmost part of the Red Sea is lower (Morcos, 1970).

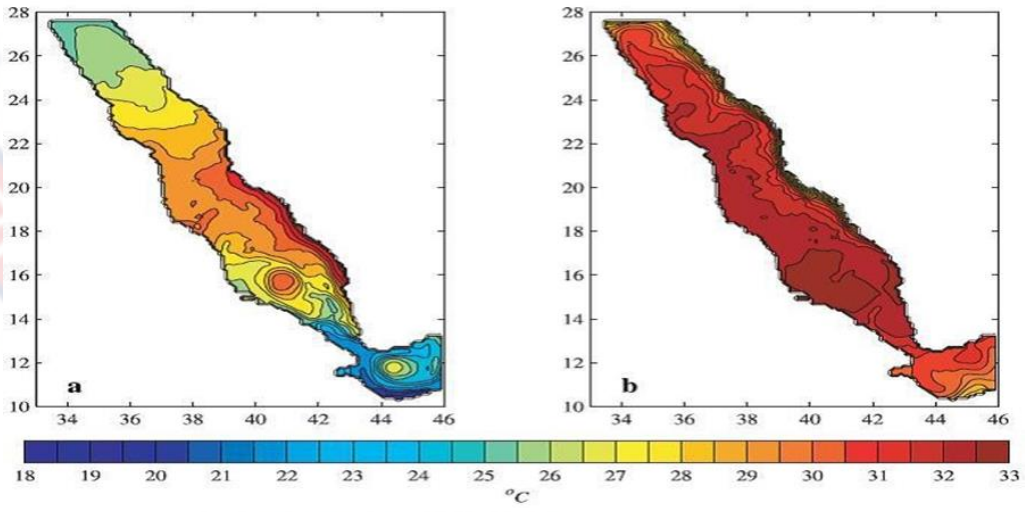

Figure 1: Seasonal SST in (a) winter and (b) summer seasons. (Sofianos & Johns, 2002).

In the southern half of the Red Sea, the monsoon wind direction has a noticeable impact on SST distribution (Madah et al., 2015). This is because the central zone experiences a weaker wind speed, where the wind converges throughout the year and is characterized by solid thermocline (Sofianos & Johns, 2002). The temperature fluctuation in the central zone is governed by the monsoon winds that blow from the northern and southern ends of the Red Sea during the winter months. In contrast, north-westerly winds predominate the whole area throughout the year (Morcos, 1970).

Because of the shallowness and the landmasses, surface sea temperatures are high near the shoreline. The Red Sea is different from tropical oceans for having a very stable warm water temperature in the deeper waters.

The vertical pattern of temperature noticeably reduces to about 23°C at about 200 m depth, and then it slowly declines to about 22°C between 200 and 300 m. The water temperature is almost constant below 300 m depth, ranging from 21.41 to 21.62°C to the seafloor everywhere. In contrast, water temperatures in most other oceans drop significantly to below 10°C at these depths (Riegl et al., 2012).

The Red Sea is categorized as one of the world's most saline water. What makes the Red Sea more saline has been apparent intriguing. The Red Sea is a semi-enclosed basin with less connection with other oceans than—so-known—meant to mix and reduce salinity. As shown in Figure 2, salinity is high in the north and decrease toward the south. In addition, high temperature signifies high evaporation, which is 2 m/yr (Sofianos & Johns, 2002), which takes up a huge amount of fresh water, making the Red Sea saltier. The Red

Sea also experiences a low precipitation rate of 2 cm/yr which is exceeded by the speed of evaporation (2 m/yr). The Red Sea lacks perennial rivers that discharge, which would supply fresh water and dilute the Sea (Sofianos et al., 2002).

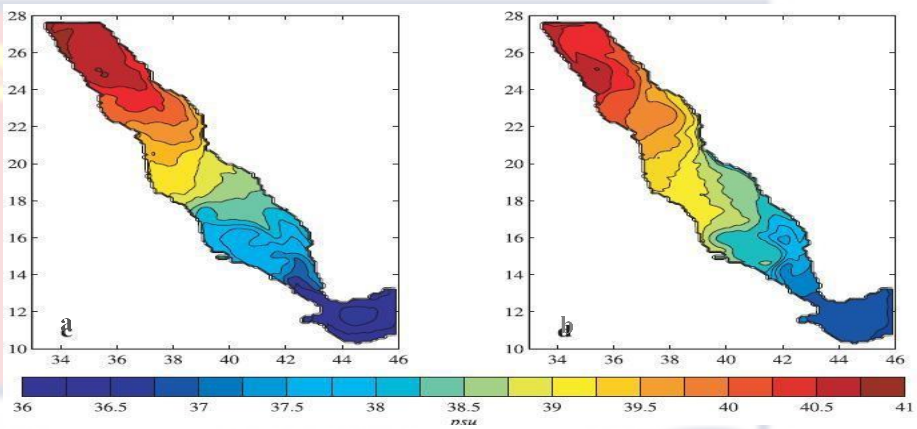

Figure 2: Sea surface salinity in winter season (a) and summer season(b) (Sofianos & Johns, 2002)

The combined effect of the temperature and salinity creates a physical barrier in the Red Sea called thermo-haline. This physical barrier acts as a barrier that prevents the mixing of the surface and deeper water. The effect of mixed layer depth is explained in the section. Usually, the Red Sea has three layers (Madah et al., 2015).

1. The mixed layer is the upper layer made from the surface towards some depth below the surface layer. This layer is deeper in Winter than in Summer. During Winter, the rising wind stress results in extending the mixed layer, while during the summer, the layer becomes shallower to about 50 m depth.
2. The thermocline layer forms beneath the mixed layer and ranges in depth from 50 to 700 m. During the winter, the thermocline layer is deepened by upward mixing caused by convective water overturning.

3. The deep layer is the lowest layer developed below the thermo-haline, and it stretches from 700 m to the floor of the sea with no variation in temperature and salinity.

The effect of surface winds and the Red Sea circulation

There are two wind patterns in the Red Sea controlled by the monsoon system. The northwest wind (Fig.3A) is prevalent in the summer season starting May to September, and the southeast wind, shown in Fig 3B is dominant in the winter season starting October to April. During the whole year, the southern region is influenced by the seasonal reversing of the monsoon wind systems. In contrast, wind direction in the northern part (roughly north of 19°N) is persistently blowing along the real axis of the Red Sea to the south partly with the effect of eastern Mediterranean weather systems, at speeds ranging between 7 – 12 km/h (Sofianos & Johns, 2002). The wind shifts from northwesterly in the summer to southeasterly in the winter on the south side of the basin, allowing water to flow into the Red Sea from the Gulf of Aden (Dreano et al., 2016; Sofianos & Johns, 2003).

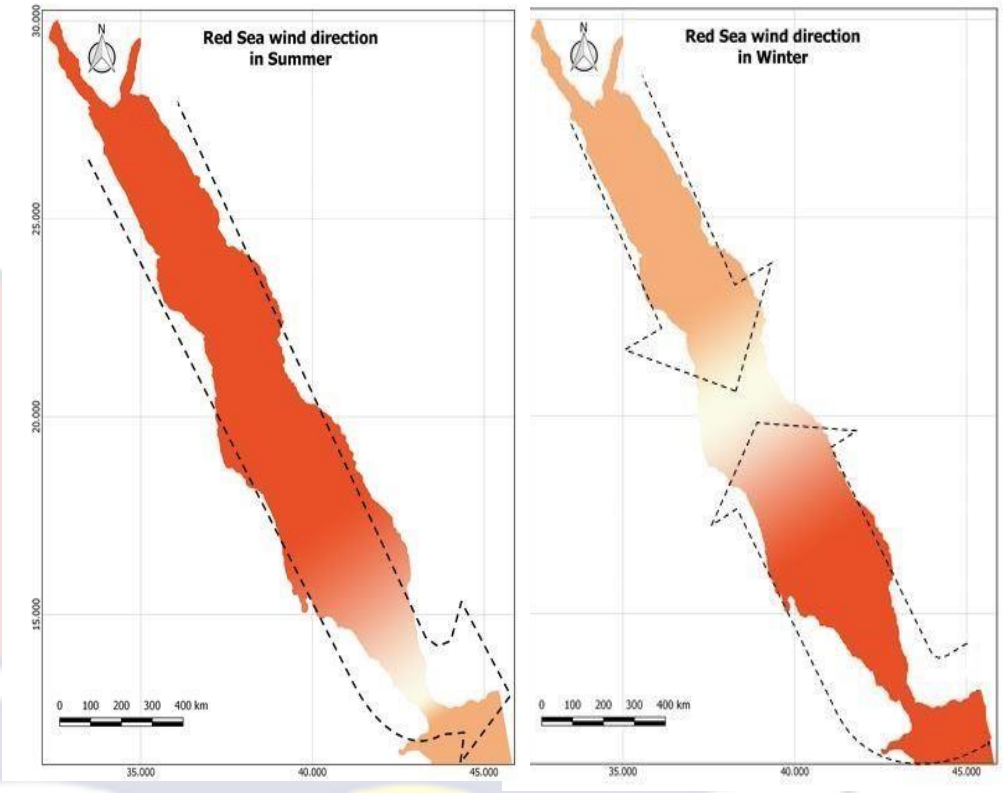

Figure 3: A general schematic representation of seasonal monsoon winds. The dashed arrow shows the wind direction, and the color intensity shows the wind energy. This map is updated and reproduced after (Sofianos & Johns, 2002).

In addition to the seasonal wind dynamics, several local controls act on the wind regime to characterize the wind variations in speed and direction. Both the eastern and western shores of the Red Sea are bounded by high mountains. The winds channeled through the gaps of the surrounding mountains on the Red Sea's sides may have large-scale effects on the surface winds, thereby controlling the direction of the winds to blow parallel to the Red Sea's longitudinal axis. Furthermore, the diurnal sea/land temperature difference affects coastal areas virtually all year, producing sea breeze during the day and land breeze at night.

Winds and density gradients in the water column, which fluctuate seasonally according to temperature, predominant winds, and evaporation, are

the primary causes of currents in the Red Sea. Previous studies conducted by researchers Neumann & McGill (1962) and Sofianos & Johns (2002) indicate that the circulation of the Red Sea and surface water movement is controlled by wind forces, thermo-haline. Furthermore, they claimed that dense water growth was caused by an excess of evaporation over precipitation. However, because the Red Sea currents are weak and unpredictable both spatially and temporally, they may help to explain why enough data isn't available. Wind has an effect at the southernmost part, particularly in the area where the Red Sea and the Indian Ocean meet at the Bab-al-Mandeb Strait. However, throughout the rest of the Red Sea region, the wind-driven circulation is significantly weaker than the thermo-haline circulation (Sofianos & Johns, 2002). The Red Sea has two distinct wind-driven circulations in the winter and summer.

1. Three-layer flow during Summer (Red Sea Surface Water, Gulf of Aden Intermediate Water—GAIW, and Bottom Red Sea Outflow Water—RSOW):

   During the summer, a thin layer of less dense (due to being heated) surface outflow water escapes the Red Sea. This is a direct effect of Northwesterly winds. GAIW, a nutrient-rich intermediate layer of water from the Gulf of Aden's upwelling zone, reaches the Red Sea and flows north to replace the Red Sea surface outflow water, sandwiched between the surface and the deeper RSOW. The third layer is the bottom Red Sea Outflow Water (RSOW), characterized by high salinity and low temperature and leaves the Red Sea below the GAIW to the Gulf of Aden (Fig.4A).

2. Two-layer flow during Winter (Gulf of Aden Surface Water—GASW, bottom Red Sea Outflow Water--RSOW): During Winter, a layer of surface water has a temperature of about 25°C and a salinity of 36.5 psu. Apparently, this enters the Red Sea from the Gulf of Aden (Gulf of Aden Surface Water) and flows north due to the influences of Southeasterly winds. Whereas the denser, a deep layer of the Red Sea water (RSOW)--having higher salinity (40.5 psu) and lower temperature (21.5°C) leaves the Red Sea outward to the Gulf of Aden (Fig.4B). As the Gulf of Aden Surface Water (GASW) continues to the north, it becomes cooler and denser mainly due to wind and high evaporation. This forces the denser water to sink dow in the northern zone to be part of the deeper RSOW, then eventually returns southward below the thermocline (250300 m depth) to the Gulf of Aden (Raitsos et al., 2013).

During Summer, the northwest winds cause the intrusion into the southern Red Sea (Yao et al., 2014). The Gulf of Aden Intermediate Water (GAIW) intrudes at a depth between the surface and deeper RSOW, moving northwards to the Farasan and Dahlak islands' shallow coral reef sections. Then, because of the shallowness of the bathymetry and local agitation, accessible nutrients may be provided to the top layers. Local mixing in the absence of GAIW, however, would not result in nutrient-rich, productive waters because ambient water bodies in the rest of the Red Sea have substantially lower nutrient contents at comparable depths (Dreano et al., 2016).

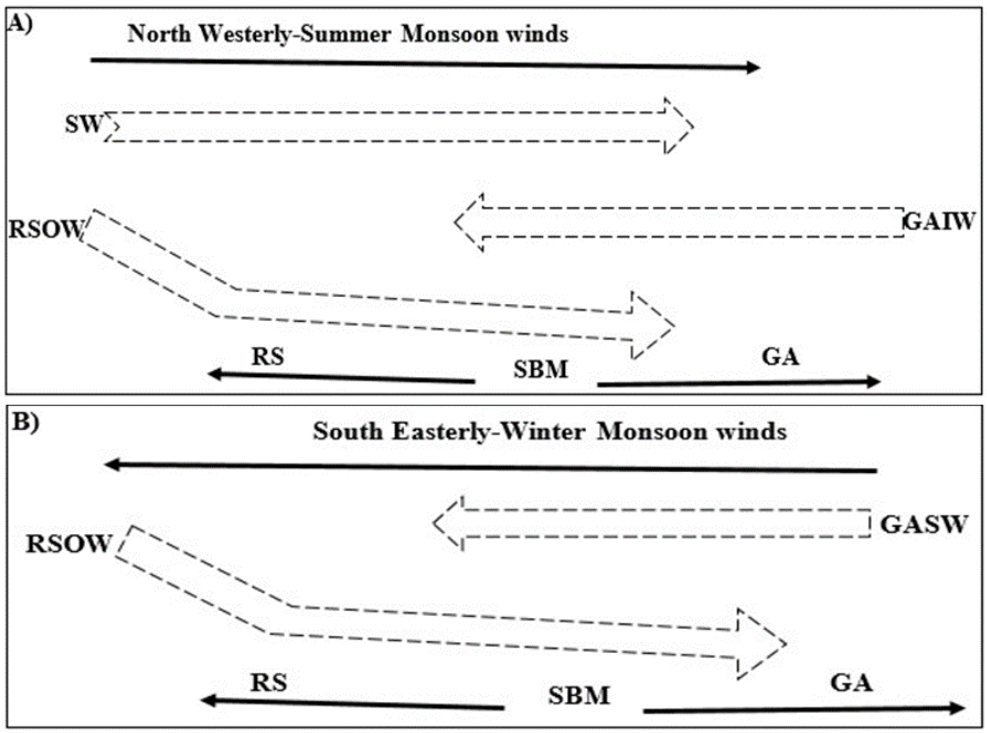

Figure 4: A Sketch of two circulation patterns in the southern Red Sea along the SBM.

Anticyclonic eddies are more common than cyclonic eddies, according to studies of Red Sea circulation (eddies and gyres) based on vessel-mounted acoustic Doppler current profiler (ADCP) data. The eddies appear to be quasi-stationary, locked in four sub-regions of the Red Sea: 17°–19°N, 19°–21.5°N, 21.5°–24°N, and 21.5°–24°N. (Sofianos and Johns 2007).

They claimed that eddies arise when positive and negative wind stress on either side of the prevailing along-axis create along-axis currents. As a result, coastal capes and promontories deflected wind jets across the basin, forming closed circulation in several Red Sea sub-basins.

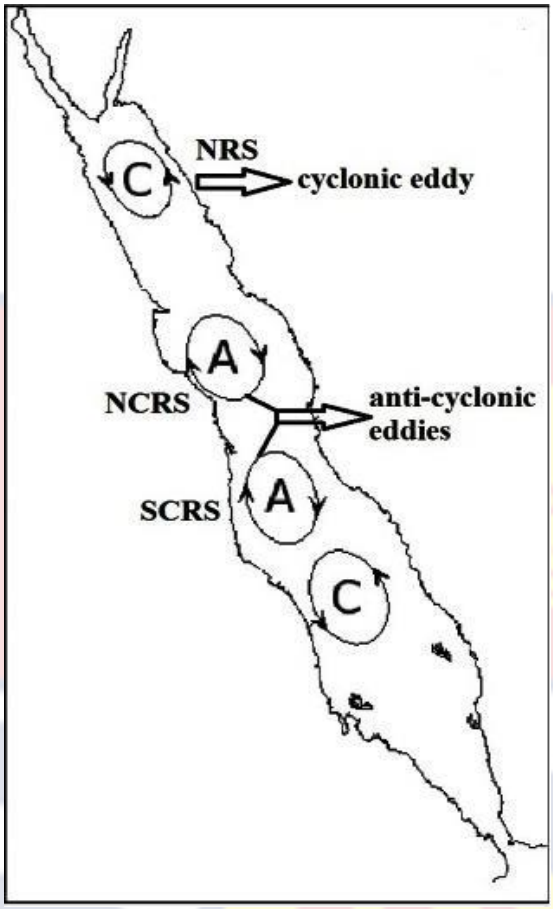

Figure 5: Schematic representation of the general circulation of the Red Sea. The main cyclonic and anti-cyclonic eddies are represented by the elliptical shapes. (Figure originally copied from Johns et al., 1999 and updated by Raitsos et al., 2013)

Chapter Summary

This chapter reviews the literature on Eritrea's and its status along the coast, as well as the ecology of coral reefs and an overview of the global situation of coral reefs.

CHAPTER THREE

MATERIALS AND METHODS

This Chapter describes the materials and methods utilized to carry out the research. The research sites are discussed in detail. Illustrations are supplied where appropriate to explain the study's methodologies. Statistical analysis techniques and software used to draw conclusions are also mentioned.

Study Site

In conducting this research, three study sites were considered around the southwest Red Sea. In the Red Sea, the Eritrean territorial water body stretches from 180°N in the north borders with Sudan at "Ras Kesar" to 12°45′N in the South-Eastern that borders Djibouti at "Ras Dumera,". The territorial waters of the Eritrean Red Sea have over 354 islands (Hilman & Tsegay, 1997). The complete coastline length is about 3300 km (1350 km of the mainland and 1950 km of island coastlines) (De Grissac & Negussie, 2007).

The Eritrean coasts and eastern swamps are portrayed by a sweltering semiarid climate that extends from 30ºC to 39ºC in June through September and decent colder weather that reaches from 25ºC to 32ºC in October through May. The islands and coastal areas have little precipitation, with a yearly average of 200 mm, and have high evapotranspiration, bringing about water shortage and decreased vegetal cover (De Grissac & Negussie, 2007).

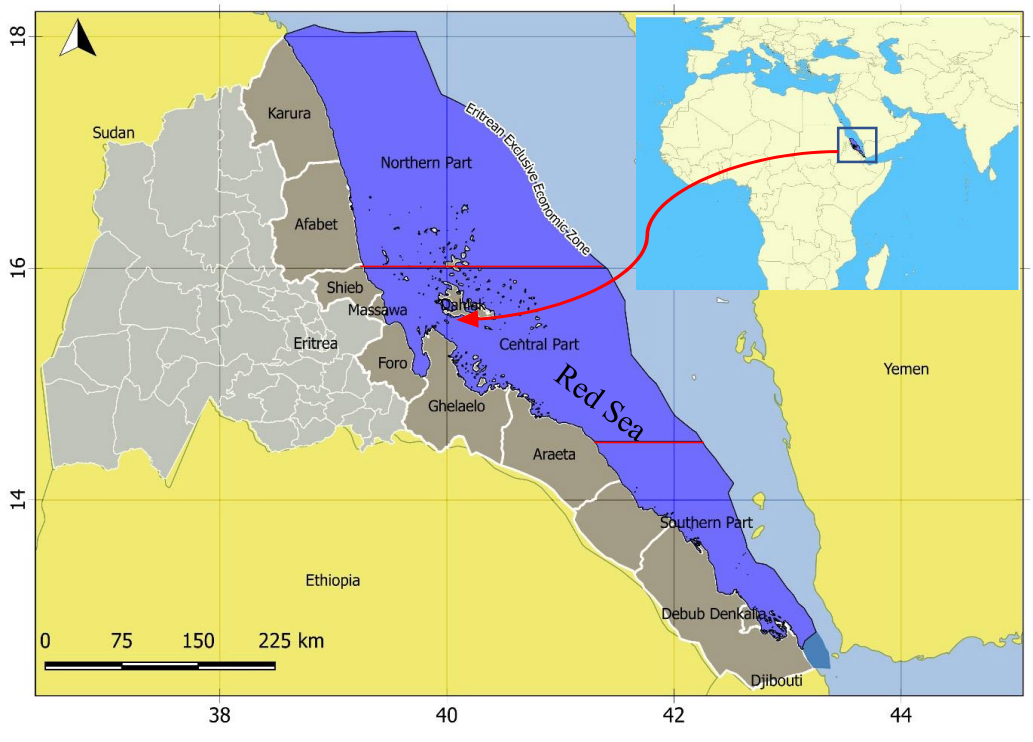

Figure 6: Map showing the whole Eritrean Red Sea. This place is studied with the help of remote sensing satellite observation.

The study considered both satellite data collection and in-situ field observation. The territorial waters of Eritrea were considered as a whole and studied using satellite observation. This was to explain the broader spectrum of environmental challenges in the region. In contrast, in-situ field observations were conducted in the Sheik Seid Island (around Massawa, Eritrea) to investigate the localized implications of environmental stressors on coral reefs.

Sheik Seid Island

Sheikh Said Island is located 1.5 km southeast of Massawa at N15°35'47.3"; E 039°27'37.4". The mangrove species *Avicenna marina* encompasses the entire island, which measures 0.12 km^2. The island's eastern side is exposed to high wave energy, whereas the western side is partially

sheltered. It is a tourist resort island that receives a lot of visitors throughout the year.

Gurgusum

Gurgusum is located at N 15º38'36.2"; E 039º28'48.4" near the old cement factory. It is a wide open reef exposed to waves and currents. The reef is located about 3km north of Massawa city therefore there are less anthropogenic impact. The reef extends a long distance parallel to the coastline.

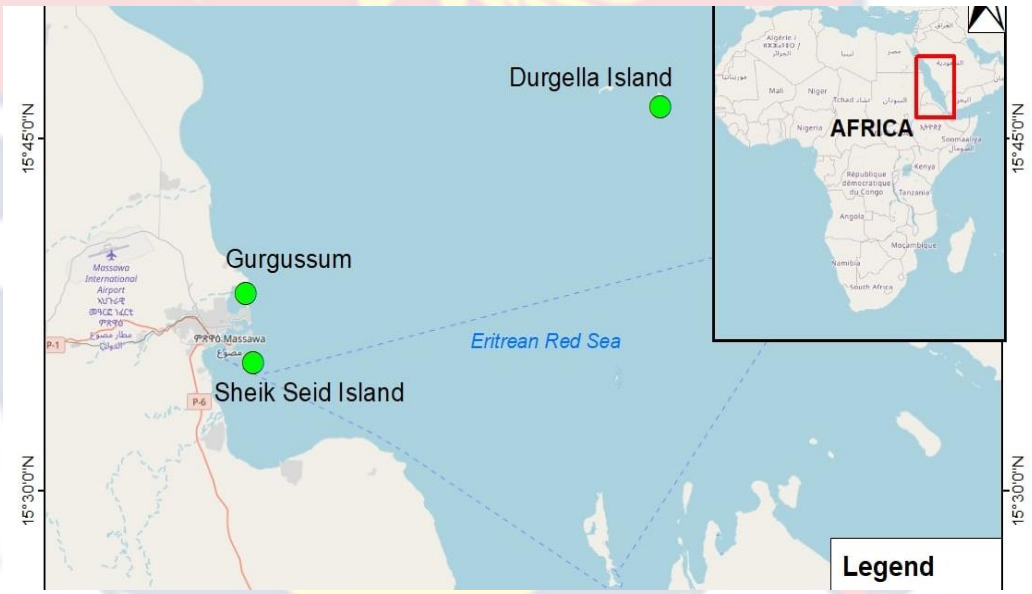

Figure 7: A study site for this study

Durgella Island

Durgella island, located at N $15^0$46'46.8"; E $039^0$47'56.4", has a total area of 1.264 km^2 and is part of the Dahlak archipelago. The outer reef and inner reef flats cover more than half of the reef, while the back reef slope and shallow lagoon cover the remaining half. The island has a few anthropogenic activities, such as the anchoring of artisanal fishermen and the area's topography is neither steep nor gentle.

Data collection

This research used data from the Sentinel2A satellite (the first of the twin polar-orbiting Sentinel-2 satellites), which falls into six categories: terrestrial, marine, and atmospheric environments, as well as climate variability, disaster management, and security, are all factors to consider. The Sentinel-2 sensors' Multi-spectral Imager (MSI) is a single optical instrument (MSI). The MSI collects 13 spectral bands in the visible-near infrared (VNIR) and short wave infrared (SWIR) ranges at three different spatial resolutions (10, 20, 60 m) (ESA, 2015).

The improved method used in this work is depicted schematically in Figure 8. Sentinel-2A multispectral image is a passive remote sensing device that monitors sunlight that has passed through the airspace, ocean waters, and seafloor and has reflected the water column and atmosphere, where a satellite sensor detects it. As a result, the initial phases of the study focused on the effects of interruptions on the fate of light in the atmosphere and water before gathering quantitative data on aquatic ecosystems, particularly coral reefs. The analysis used Sentinel-2A bands 2, 3, 4, and 5 (except for Near-infrared band 8 to mask out the land), and band five was resampled by band two from 20 m to 10 m, which penetrated the water column deeper and provided practical quantifiable information on bottom reflectance values.

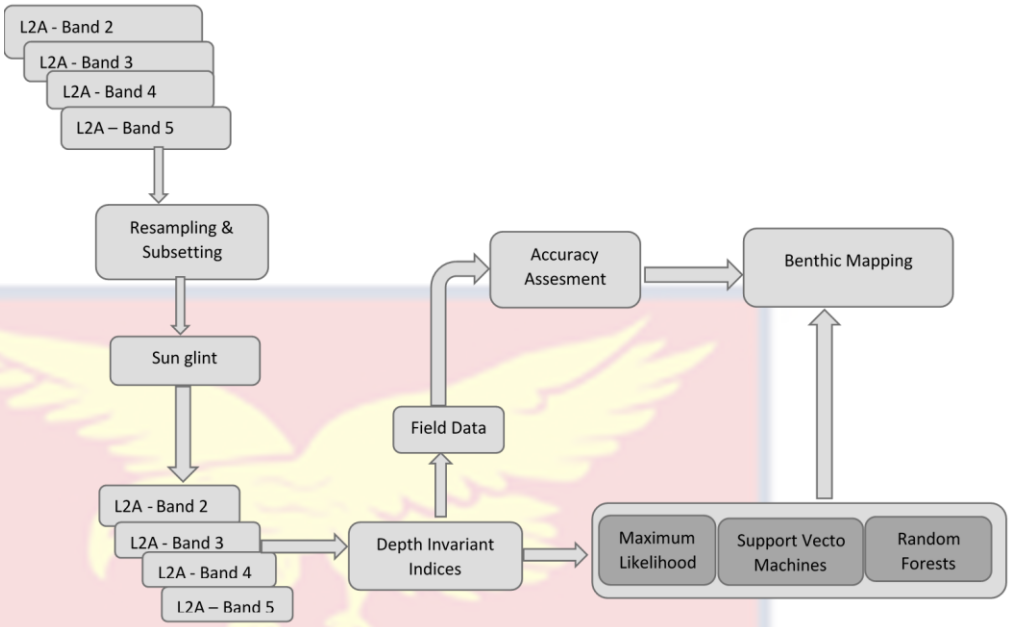

Figure 8: Schematic presentation of the methodology.

To conduct this investigation, Sentinel-2A image taken at 9:09 a.m. UTC on March 27, 2020, were processed and analyzed (Table 1). The image data was retrieved from Sentinels Scientific Data Hub (https://scihub.copernicus.eu/), which provides free Sentinel-2 Level-1C (L2A) user products. The tile labeled S2A MSIL2A 20200327T074611 N0214 R135 T37PET 20200327T103448.data (Table 1) was chosen for further investigation of study sites.

Table 1: Sentinel-2A image characteristics

Tile – ID	
S2A_MSIL2A_20200327T074611_N0214_R135_T37PET 20200327T103448	
Acquisition date	27 March 2020
Acquisition time	07:46:11.024000
Sensor view zenith angle	25.4344362658664
Sensor view azimuth angle	124.194395667339

Remote sensing data frequently necessitates correct site information to improve visual representation and feature selection, enable supervised classifications, and predict specific accuracy assessment. Due to a multitude of characteristics that can induce spectral misunderstanding, i.e., water quality, depth gradient, and habitat variety were all factors to consider. To address this, a stratified random selection technique was created to ensure a fair assessment of all physical ecosystems throughout their various depth ranges (Congalton, 1991).

Image Masking

Image masking is an essential part in remote sensing because it improves the visibility of coastal water features by masking land features. The original granule was clipped to the coastal research region using near-infrared (NIR) band 8, masking over the land and deeper seas more than 20 m. It was necessary to retrieve solid quantitative estimates of the seabed. Due to the extremely high-water absorption at that wavelength, NIR Band 8 was chosen. Using an Iso Cluster Unsupervised Classification, the Sentinel-2A granule was classified into two classes: land and water. The masked research area was then extracted using the water class.

Image Classification

Maximum Likelihood Classifier

The Maximum likelihood classifier (MLC) calculates the probability that a given pixel belongs to a specific category under the assumption that each class in each band is normally distributed. A pixel's possibility of belonging to a specific class is compared, and the pixel in question is allocated to the class with the highest probability (i.e., maximum likelihood). If a

probability threshold is set and the highest probability is less than it, the pixel stays unclassified.

Suppose there are N classes represented by C_i, where $i = 1, \dots, N$, that a given pixel can potentially be assigned. The conditional probability of a given pixel with measurement vector x is denoted by $P(C_i|x), i = 1, \dots, N$. The MLC assigns the candidate pixel x (pixel with values x) to class C_i if the conditional probability for class C_i is higher than the rest, i.e.,

$$P(C_i|x) \geq P\left(C_j|x\right) for\ all\ j \neq i.$$

Equation 1

An MLC is a supervised classifier, and hence labeled data is used to train it. During the training, the conditional probabilities (likelihoods), $P(x|C_i), i = 1, \dots, N$, are estimated, and Bayes' rule is used to calculate the conditional probabilities used in the decision rule of the MLC. The Bayes' rule is:

$$P(C_i|x) = \frac{P(C_i)P(x|C_i)}{P(x)}$$

Equation 2

where $P(C_i)$ represents the probability of a pixel from category C_i can be spotted anywhere on the map, and $P(v)$ is the probability of seeing a pixel with information vector v in the map.

The probabilities, $P(x|C_i)$, are computed using a multivariate normal probability density function given by

$$P(x|C_i) = \frac{1}{(2\pi)^{\frac{N}{2}}|\Sigma|^{\frac{1}{2}}} \exp\left\{-\frac{1}{2}\left(x - \bar{x_i}\right)^T \Sigma_i^{-1}(x - \bar{x_i})\right\}$$

Equation 3

where $\bar{x_i}$ is the mean vector of class C_i, and Σ is the variance-covariance matrix of class C_i.

Because of its ease of adaptation and widespread use in remote sensing studies of shallow aquatic ecosystems, the maximum likelihood classifier (MLC) was chosen for this study.

Random Forest Classifier

Random forest (RF) is a supervised learning algorithm used for classification. RF solves a classification problem by combining several decision trees, each producing a unit vote for the most popular class to classify an input vector. Each decision tree is trained independently using bootstrapped samples (features), and the Gini index was used to determine the best split selection (Breiman, 2001) at each node. These classifiers increase the model's efficiency by combining predictions to form a "forest" (Breiman, 2001). Due to their robustness to outliers, noise, correlation, and firm performance with small datasets, the random forest has been widely used to classify remote sensing data (Gislason et al., 2006).

In the process, the user must specify the number of decision trees to grow and the number of features m to be sampled randomly from the total number of features p. In this study, the number of bootstrapped samples was taken as $m = \sqrt{p}$, and the number of decision trees to grow was specified to be 100. For random forest parameterization, the EnMAP-Box software was also employed.

Support Vector Machine Classifier

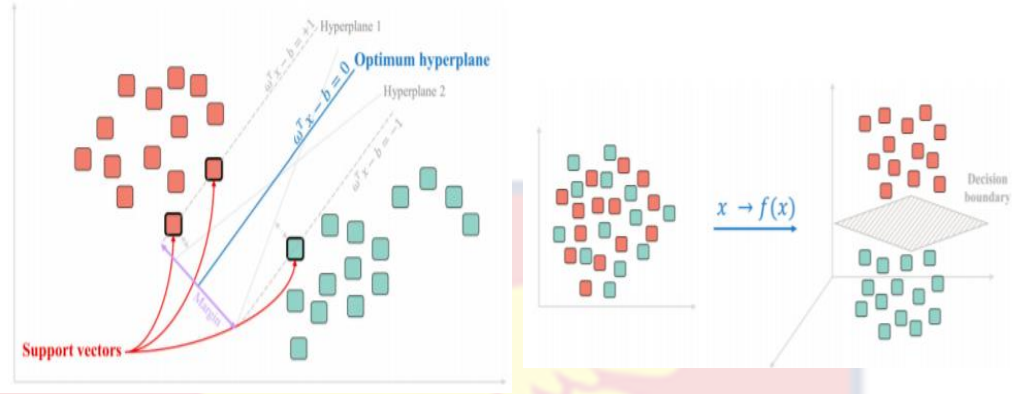

Figure 9: Support Vector Machine (SVM) classification for 2-dimentional data using an optimum hyperplane in 3-dimension.

Support Vector Machines (SVM) are one of the most used supervised classification algorithms to separate two classes by finding an optimal separating hyperplane (decision boundary). The closest samples to the decision boundary are called support vectors. One of the advantages of SVM is that they can be used for linearly and/or non-linearly separable classes. To find a hyperplane for non-linearly separable classes, SVM employs a kernel function. The goal of a kernel function is to project (map) the available feature space into a higher-dimensional space to identify the best optimal class separation hyperplane.

For this research, the Gaussian radial kernel function was used when applying SVM to the training data. The radial kernel basis is given by,

$$K(x, x_i) = \exp\left(-\gamma||x - x_i||^2\right)$$

Equation 4

where $\gamma > 0$ is a constant that defines the width of the data, x^* is the candidate pixel measurements vector, and x_i is the measurement vector for pixel i.

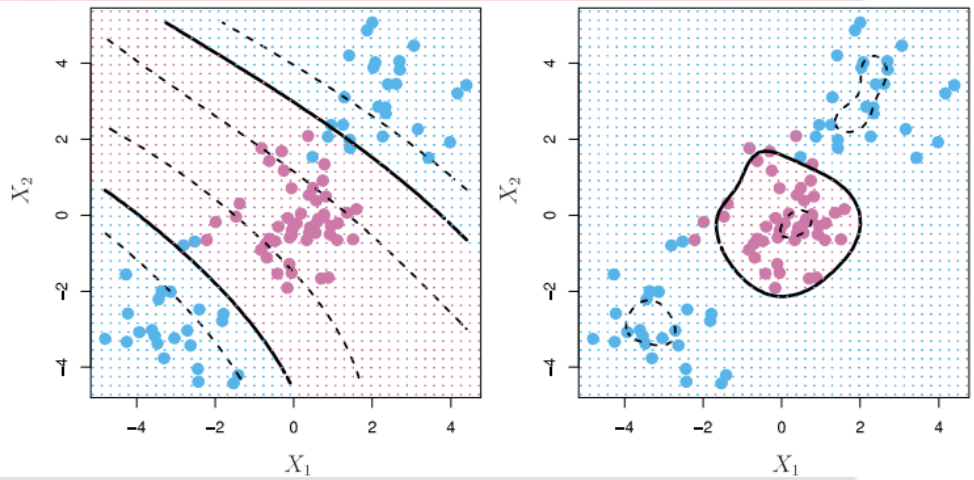

Figure 10: (a) SVM with a polynomial kernel function (on the left-hand) and (b) a radial kernel function (on the right) in classifying two-dimensional data.

Accuracy Assessment

The accuracy evaluation stage is critical in remote sensing because it verifies the accuracy of image class (i.e., generating habitat maps) and establishes the relationship between images and realities. The accuracy evaluation is based on the error matrix. Therefore, error matrices were constructed for the image classifications. It consists of a square array of rows and columns, each row and column representing one of the classification's habitat classes. The number of classified training samples is represented by each cell in the error matrix. Simultaneously, the showing various classified training data and the columns indicate reference data for evaluating the classified data.

Benthic Coverage

The percentage cover of corals in the area was determined using the Line Intercept Transect (LIT) method given by (Loya, 1972; English et al., 1997) in comparison to other benthos. Data was collected via snorkeling at a depth of roughly 2 - 3 m. A measuring tape was laid along marked transects, and the presence of various genera as well as intercept distances in centimeters for each category were recorded on an underwater slate. This is the most used technique for monitoring benthic organisms (Steingrimsson, 2005). A 10 m transect line was chosen to obtain an unbiased estimate of cover; this has previously been demonstrated to be an adequate sample size for a quantitative study of hermatypic corals (Loya, 1972; Beenaerts & Berghe, 2005). The substrate was classified as live coral, dead coral, crustose coralline algae, sponges, rubble, sand, and other invertebrates. Furthermore, coral identification books were used to identify scleractinian corals up to the genus level (Veron, 2002). The above-mentioned category's percentage coverage was computed.

Coverage comparison

Multivariate analysis of variance (MANOVA) is a statistical technique used to compare the means of two or more groups on multiple continuous dependent variables. In the context of benthic coverage, MANOVA can be used to examine differences in the proportions of different types of benthic organisms (e.g., live coral, dead coral, algae, sponges, rubble and sand) among different sites and between years. By analyzing multiple dependent variables simultaneously, MANOVA allows for a more comprehensive assessment of differences in benthic coverage than univariate methods. MANOVA can also

be used to test interactions between site and year, which can provide insight into how benthic coverage varies across time and space.

For statistically significant differences resulted from the MANOVA, a Tukey's Honestly Significant Difference (HSD) post hoc test, statistical test that is conducted after a primary analysis, such as MANOVA, to determine which groups differ significantly from one another, was performed. The purpose of a post hoc test is to identify specific differences between groups that were not detected by the primary analysis. This is important because MANOVA only determines whether there is a statistically significant difference between groups, but it does not indicate which specific groups are different from each other.

Sea Surface temperature (SST) for the years 1986 - 2020

A variety of approaches can be used to estimate SST at different levels of the ocean's near-surface thermal structure. This is related to the two types of SST: skin SST (the temperature at the top few micrometers of the sea surface) and sub skin SST (the temperature a short distance (1 mm) from the surface).

SST data were downloaded from NOAA coral reef watch on-board from the NOAA coral reef watch website, https://coralreefwatch.noaa.gov/product/vs/data/, on a daily basis for the years 1986 through 2020. To follow the temperature conditions required in coral bleaching and quantify the intensity of bleaching stress globally, NOAA began publishing web-accessible, satellite-derived, global near real-time nocturnal SST products. NOAA SST is acquired in level 3 (L3) in spatial resolution of ≈5 km. SST data are collected from a variety of sensors (e.g., thermal infrared, microwave) on both polar-orbiting and geostationary satellites. The NOAA

SST is in Celsius (°C). The L3 products are produced daily for night conditions.

During the study period, SST in-situ data was collected using HOBOware data loggers. Two HOBOware temperature loggers were deployed at 1m depth around the Massawa coasts near Sheik Seid Island and Gurgusum. Beginning in January 2013, the loggers automatically recorded temperature at 30-minute intervals. Finally, the data collected in the memory of the data loggers was downloaded and analyzed using the HOBOware Pro software.

Normalized anomalies (differences from the time series mean) were calculated for each dataset to determine rate of change, consistency, and direction. The seasonality effect was effectively removed from the time series using this method. The Mann–Kendall monotonic trend statistic, a non-linear metric, was used to determine trend direction and change constancy. The Mann–Kendall statistic ranges from -1 to +1; negative value indicates a decline whereas a positive value is an indication of rising trend.

Autoregressive Integrated Moving Average (ARIMA Model)

It is well studied that non-stationary data can be made stationary by differencing. Differencing consecutive values is intended to remove trend and differencing values at different times of the same season are aimed at removing seasonality. A non-seasonal autoregressive integrated moving average (ARIMA) model is a model that incorporates consecutive value differencing and combines an autoregressive (AR) model of order p given by

$$y_t = c + \phi_1 y_{t-1} + \phi_2 y_{t-2} + \cdots + \phi_p y_{t-p} + \epsilon_t, where\ \epsilon_t \sim WN(0, \sigma^2)$$

Equation 5

and a moving average (MA) model of order q given by

$$y_t = c + \epsilon_t + \theta_1\epsilon_{t-1} + \theta_2\epsilon_{t-2} + \cdots + \theta_q\epsilon_{t-q}, \qquad \epsilon_t \sim WN(0, \sigma^2).$$

Equation 6

Both AR(p) and MA(q) models are used when the time series data is stationary (no seasonality or trend).

The mathematical model of an $ARIMA(p, d, q)$ is given by,

$$y'_t = c + \phi_1 y'_{t-1} + \cdots + \phi_p y'_{t-p} + \epsilon_t + \theta_1\epsilon_{t-q} + \cdots \theta_q\epsilon_{t-q}.$$

Equation 7

where y'_t is the differenced value, p is order of the AR part, q is order of the MA part and d is degree of first differencing. Using a backfit notation, the Equation 7 can be written as

$$\left(1 - \phi_1 B - \cdots - \phi_p B^p\right)(1 - B)^d y_t = c + \left(1 + \theta_1 B + \cdots + \theta_q B^q\right)\epsilon_t$$

Equation 8

The backshift operator is given by $By_t = y_{t-1}$, $B^2 y_t = y_{t-2}$, …, $B^p y_t = y_{t-p}$.

A seasonal ARIMA model, $SARIMA(p, d, q)(P, D, Q)_m$, incorporates seasonal differencing into a non-seasonal ARIMA model.

$$\text{ARIMA} \quad \underbrace{(p, d, q)}_{\text{Non-seasonal part of the model}} \quad \underbrace{(P, D, Q)_m}_{\text{Seasonal part of the model}}$$

where m is the number of observations per year.

Without loss of generality, assuming the value of all the operators (p, d, q, P, D, and Q) as one, and m=12, an $SARIMA$ model can be written with the backshift operator as

$$(1-\phi_1 B)(1-\Phi_1 B^{12})(1-B)(1-B^{12})y_t = (1+\theta_1 B)(1+\Theta_1 B^{12})\epsilon_t$$

Equation 9

where ϕ_1, Φ_1, θ_1 and Θ_1 are parameters of the model to be estimated from the data and B is a backshift operator. In Equation 9, the constant term is omitted for simplicity.

The 'statsmodels' python module was used to fit a *SARIMAX* model to the SST data through a grid search.

Effect of temperature and Chlorophyll-a concentration on coral reefs around the central region

First, the dataset for Chl-a were downloaded in NetCDF format globally. These datasets were opened in python by using netCDF4.Dataset function under the netCDF4 package. All images were rasterized using the raster function, and after that, the data was projected into WGS 84 using the proj4string function. Then the data became compatible and overlaid with the shapefile of the southern Red Sea with WGS 84 projection. Therefore, the global data was cropped into the study area of interest in the southern Red Sea using crop function. For Chl-a datasets, the daily images of each month were merged into a single image using merge. A single image was plotted for each month by using plot. Likewise, the SST datasets (in a daily basis) were merged (composite) to give daily average images.

Chlorophyll-a (Chl-a) Algorithm

According to the OC-CCI product user guide v3.1, the dataset is created by band-shifting and bias-correcting MERIS, MODIS, and VIIRS data to match SeaWiFS data, then producing per-pixel uncertainty estimates. Furthermore, these data sets are binned to level 3 (L3) with a spatial resolution

of 4 km to map daily with a better spatial and temporal resolution. All latitudes and longitudes are given in WGS/84 datum, and the primary projection used in the OC-CCI processing chain is a globally sinusoidal equal-area grid, which corresponds to the NASA standard level 3 binned projection [RD 3]. The output datasets have the advantage of providing better spatial coverage and better results than an individual sensor.

Chl-a is measured in mg m-3 of water in OC-CCI products in the CCI-user survey, chlorophyll-a concentration was chosen as an Essential Climate Variable.

Degree Heat Week (DHW) effectiveness as a coral bleaching index based on bleaching occurrence/non-occurrence during temperature fluctuations.

Three sites in the southern Red Sea along (N15°35'36.9"-E39°47'56.4") were chosen to confirm the degree heat week using observed bleaching events: Sheik Seid and Gurgusum along the Massawa Region in the Eritrean coast's central west coast, and Durgella around the Dahlak archipelagic islands (Figure 7). Massawa was classified as a port when it came under Ottoman authority in 1557, and it is Eritrea's first port that is still operational today. To characterize historical temperature conditions throughout the selected sites, use the coordinate points mentioned above (Figure 6). Daily SST data for a 5 km grid for the selected site was obtained from the Coral Reef Watch Temperature Anomaly Database from Easier access to scientific data (ERDDAP) for the period 1986–2020, avoiding land interference. Three pre-calculated measures were obtained from the ERDDAP coral reef using the pandas' package in Python statistical analysis, as reported in (Liu et al., 2006): (1) daily SST (°C, i.e., absolute daily SST values), (2)

daily SST Anomalies (SSTA, °C); i.e., deviation from the daily SST long-term mean (1986–2020), and (3) daily Thermal Stress Anomalies Degree Heating Weeks. In particular, the cumulative SST over a 12-week sliding window where SST exceeded the threshold (Liu et al., 2006). The long-term monthly mean SD for each location was utilized to calculate the maximum/minimum climatology range (i.e., ultimate summer/winter mean) as well as the long-term seasonal variation/fluctuation (i.e., maximum minus minimum climatology). The maximum climatology +1°C heat threshold for coral bleaching was calculated (Selig et al., 2010).

The coral bleaching Degree Heating Weeks (DHW) data from the coral reef watch (CRW) https://coralreefwatch.noaa.gov/product/5km/index.php daily global 5km satellite product calculates the cumulative heat stress experienced by coral reefs over the past 12 weeks (3 months). While the daily global 5 km satellite Coral Bleaching Hotspot provides an instantaneous assessment of heat stress, Glynn & D'Croz (1990) discovered that corals are susceptible to cumulative heat stress. To track the cumulative effect, CRW developed the coral bleaching DHW heat stress index in 2000. CRW chose to accumulate Coral Bleaching Hot - spot values equal to or greater than one degree Celsius, despite Glynn (1990) establishing that temperatures greater than one degree Celsius above the average summertime high (i.e., the bleaching threshold temperature) are sufficient to cause stress, including bleaching, in corals. While the daily global 5 km satellite Coral Bleaching Hotspot provides an instantaneous assessment of heat stress, Glynn & D'Croz (1990) discovered that corals are susceptible to cumulative heat stress. The DHW formula is in the table below. The DHW value for a specific day I

(DHW_i) was calculated using this mathematical equation as the sum of 1/7 of each Coral Bleaching HotSpot (HSj) value of 1°C or higher within a 12-week (84 days) running window up to and including that day (i). Since the duration of coral bleaching is frequently on the order of weeks, the final DHW value is expressed in degrees Celsius-weeks (°C-weeks) using a factor of $\frac{1}{7}$.

$$DHW_i = \sum_{j=i-83}^{i} \left(\frac{HS_j}{7}\right), \ where\ HS_j \geq 1$$

Equation 10

To investigate the spatial variation in thermal history measurements, one-way ANOVA was used, and to check the normality of the data, Tukey's post hoc analyses with the Shapiro test (i.e., annual mean of daily SST, SST anomalies, and annual max DHW). GLMs (generalized linear regression models) were used to determine the trend of SST annual means, SST anomalies, and maximum yearly DHWs at each site over 34 years of study (1986–2020). To determine the amount of DHWs and how they fluctuated over spatial and temporal, all yearly max DHW data from 1986 to 2020 were separated into size bins that represent the likelihood of bleaching severity: (1) sub-lethal stress > 0 but < 4°C-weeks, (2) considerable bleaching >4 but <8°C-weeks, and (3) extensive bleaching high mortality at > 8°C-weeks extensive bleaching high mortality (Liu et al., 2006).

CHAPTER FOUR

RESULTS

This chapter organizes and presents information gleaned from various field studies and observations. In this chapter, data analysis outputs such as descriptive and inferential statistics are presented. Furthermore, the facts and comments have been organized and presented in accessible tables, charts, diagrams, and photos. Unless otherwise stated, standard error (SE) numbers and bars were used to show means in tables and charts 95% confidence interval was used for statistical tests of differences, and the commonly used significance level of 0.05 was considered in drawing conclusions. Regular/superscript alphabets have been used to express significant differences in graphs and tables to aid comprehension.

Image classification

The raster data for the five class habitat maps of the Massawa region study site was subjected to three different supervised classifiers: Maximum Likelihood, Support Vector Machine, and Random Forests. The accuracy of the three habitat maps was assessed using 136 in situ points and is represented by the error matrix. Figure 11 portrays the habitat mappings for each of the imagery resulted from the classification techniques under consideration are shown in Figure 11.

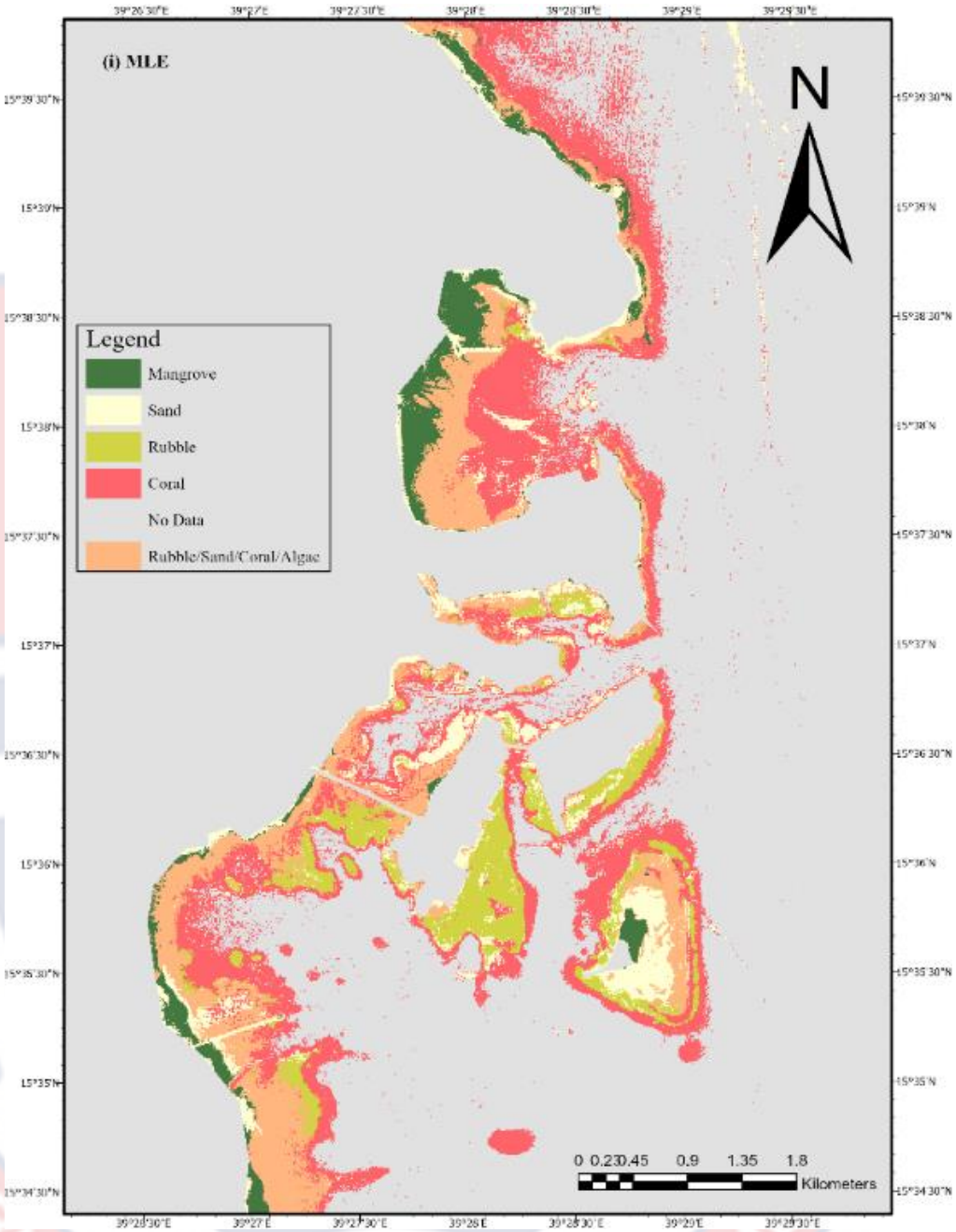

Figure 11(i): (Classification of Sentinel-2A RGB data, (i). Maximum likelihood estimation (MLE) classification. In the UTM (zone 34) system and WGS84 Projection

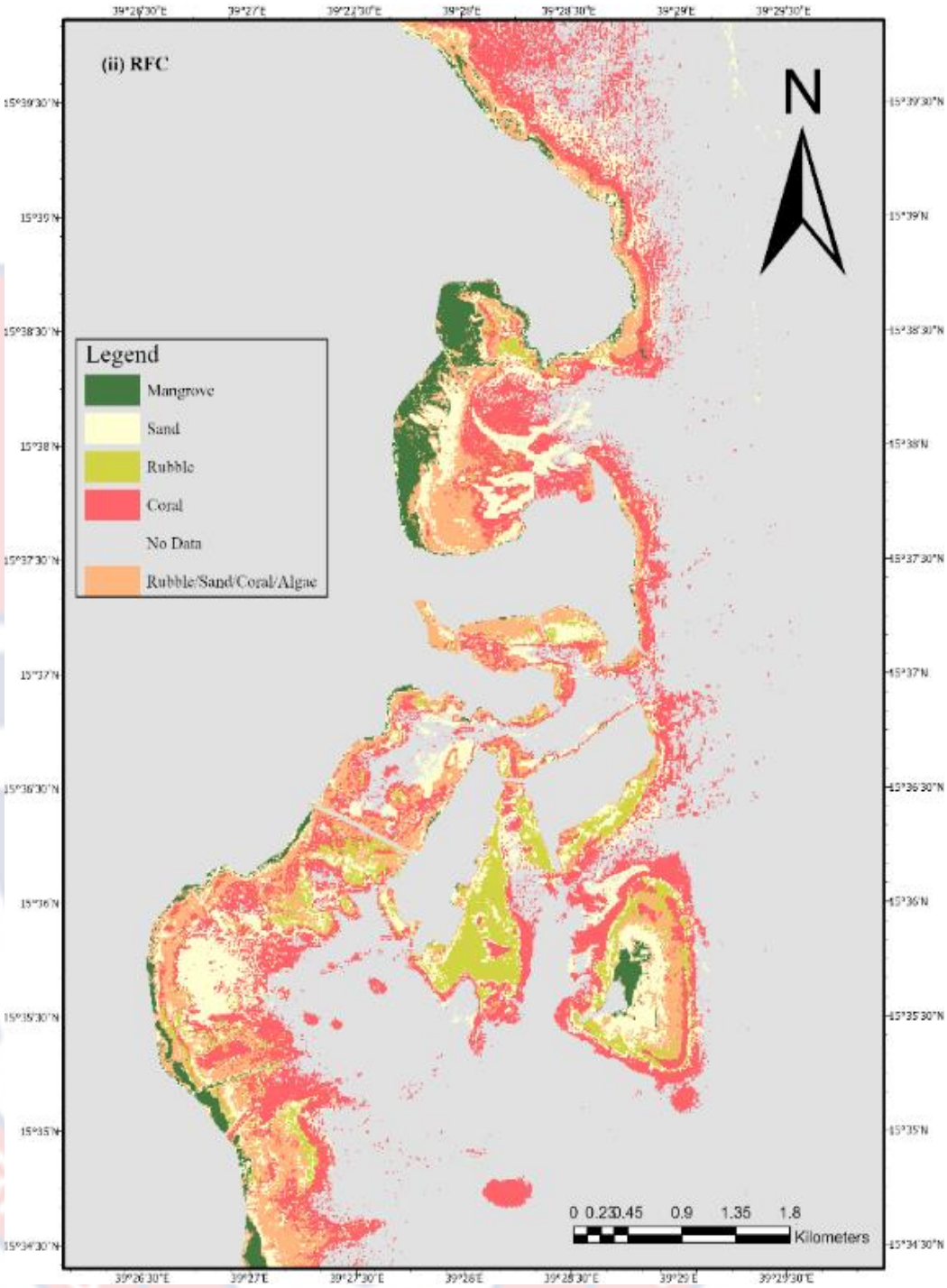

Figure 11(ii): Classification of Sentinel-2A RGB data, (ii). Random Forest classification. In the UTM (zone 34) system and WGS84 Projection

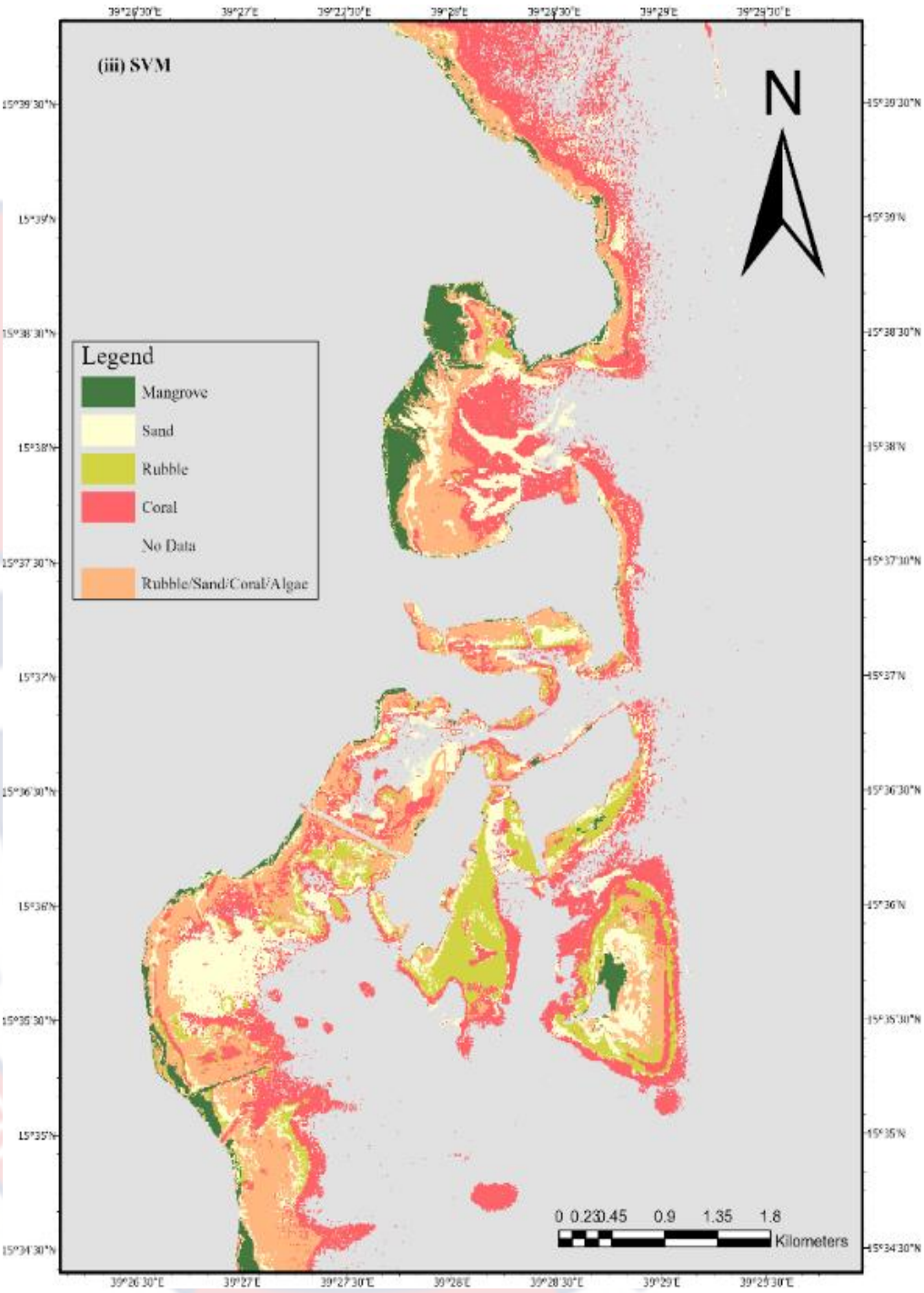

Figure 11(iii): Classification of Sentinel-2A RGB data, (iii). Support Vector Machine (SVM) classification. In the UTM (zone 34) system and WGS84 Projection

Support Vector Machine classifier produced an overall accuracy of 74% which is higher than that of the others. The error matrices for the SVM classifier for the imagery composite are shown in Table 2.

Table 2: SVM Classification accuracy metrics

Classes	**Coral**	**Mangrove**	**Rubble**	**Sand**	**Deep Water**	**Coral/ Rubble/ Sand/ Algae**	**Total**	**User Accuracy %**
Coral	51	0	2	2	0	2	57	89.5
Mangrove	0	8	0	1	0	0	9	88.89
Rubble	7	0	9	2	0	4	22	41
Sand	3	0	1	14	0	1	19	73.7
Deep water	1	0	0	0	13	0	14	92.9
Coral/ Rubble/Sand/ Algae	7	1	2	3	0	12	25	48
Total	69	9	14	22	13	19	146	
Producer accuracy	73.91	88.89	64.28	63.6	100	63.1579		
Overall accuracy: 74%, Overall kappa coefficient: 0.65								

The live coral covers an area of 5.07 km^2 at depths ranging from 1 to 5 m, with a mean presence of 2 m, according to satellite-derived mapping of the Massawa region. Overall, live corals occupied 14.3% of the total surveyed area of 36.23 km^2. The total benthic categories of the Massawa region, according to the best classifier, are approximately 13.94 km^2. Figure 12 shows that live coral accounted for 36% of the total coverage, with rubble/sand/ coral/algae for 25%, Mangrove for 7%, and sand and rubble accounting for 22% and 10%, respectively.

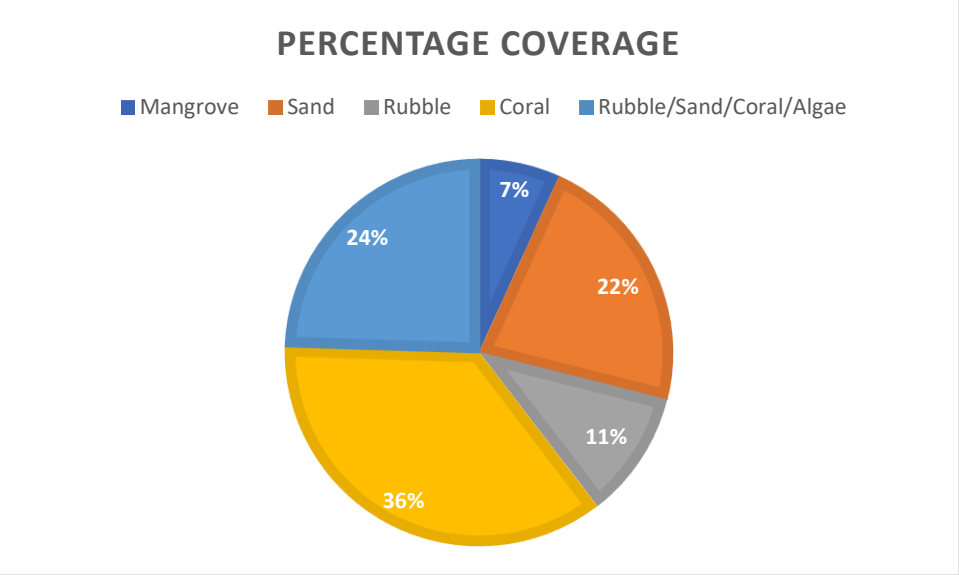

Figure 11: Area coverage of benthic categories maps around Massawa.

Sea Surface Temperature (SST) historical changes

SST samples collected in the coral reef between January 1986 and December 2020 were made up of daily SST records from three different locations. Figure 12 depicts the SST historical data for the three named sites. The temperature reaches its highs (>30^{o}C) during the summer and its lows during winter. We expect historical sea surface temperature to differ based on the location of the sites, with anthropogenic effects expected to increase but all sites increasing dramatically in recent years.

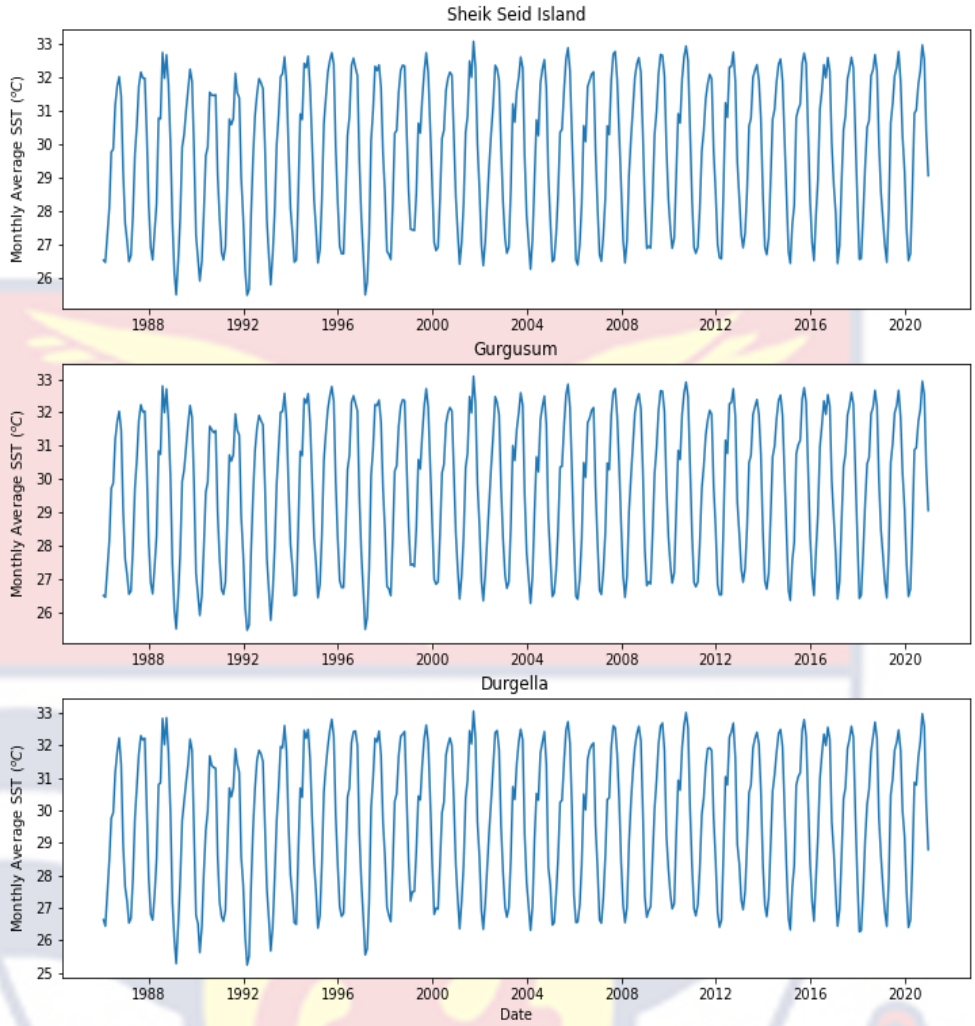

Figure 12: Monthly average sea surface temperature for three different sites.

Sea Surface Temperature Anomaly (SSTA)

SSTA was calculated by subtracting the daily SST value from the long-term average SST data for a specific site and day of the year. A positive anomaly in Figure 13, indicates that the SST is warmer than average, whereas a negative anomaly indicates that the SST is cooler than the maximum monthly mean.

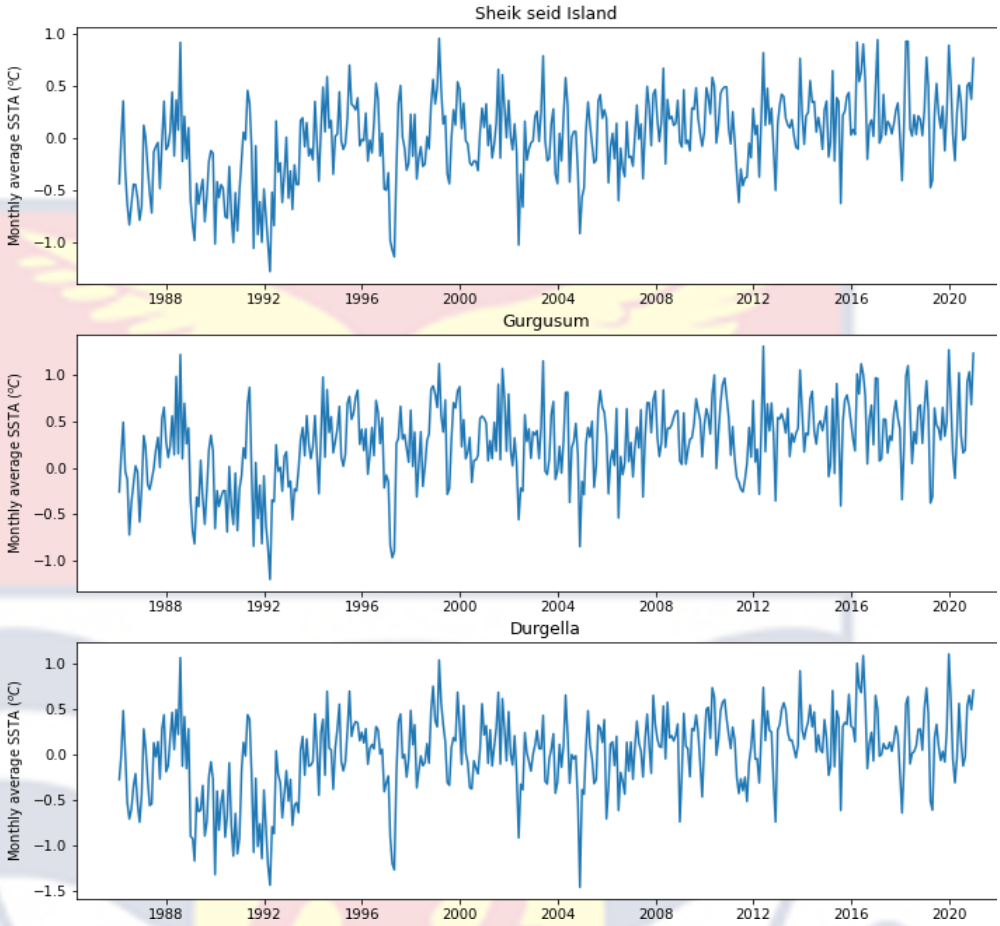

Figure 13: Monthly average sea surface temperature anomaly.

Visually inspecting Figure 13 and Figure 14, it may is not clear if a trend exists in the SST and SSTA data. Decomposing the data into its seasonal, trend, and error components allows us to examine these details separately. Figure 15 presents the trend component of SST and SSTA data. In both plots, a trend appears to exist.

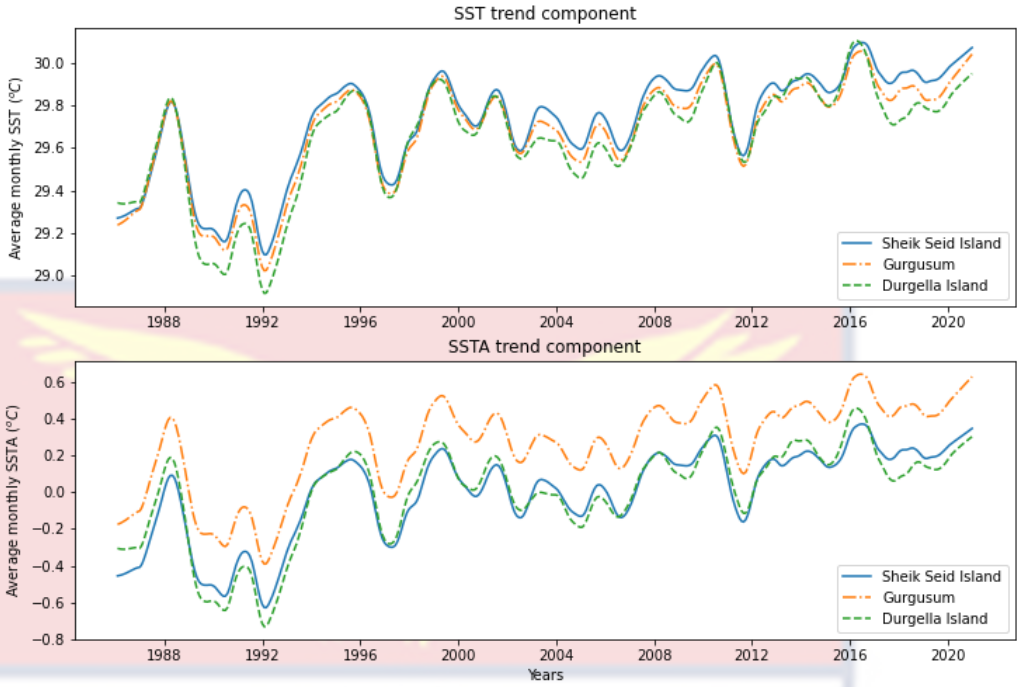

Figure 14: SST and SSTA trend components after removing seasonality.

The significance of the trend was tested using the Mann-Kendall trend test and the results for the SST data are presented in Table 3. The results show that in each of the three study sites, a statistically significant uprise of SST was seen in the years under consideration. Moreover, the Mann-Kendall test results for the SSTA data are identical to the data presented in the Table 3.

Table 3: Mann-Kendall trend test for SST data

Site	Tau value	p-value	Slope	Intercept	Trend
Sheik Seid Island	0.3017	<0.0001	0.0173	29.9026	Increasing
Gurgusum	0.2835	<0.0001	0.0164	29.9037	Increasing
Durgella Island	0.2503	<0.0001	0.0157	29.7535	Increasing

The best fit model was found to be a *SARIMA (1,1,1)(0,1,1)*. The result is given in Table 4. Changing the value of the order P to zero, Equation 9 can be written as

$$(1-\phi_1 B)(1-B)(1-B^{12})y_t = (1+\theta_1 B)(1+\Theta B^{12})\epsilon_t$$

Equation 11

Substituting the estimated values provided in Table 4, and multiplying all the factors, Equation 11 can be expressed as

$$y_t = 1.3625y_{t-1} - 0.3625y_{t-2} - y_{t-12} + 1.3625y_{t-12} - 0.3625y_{t-14} + \epsilon_t$$
$$- 1.0583\epsilon_{t-1} - 1.0583\epsilon_{t-12} + 1.0286\epsilon_{t-13}$$

Table 4: Seasonal ARIMA model fitted to SST data.

SARIMAX Results

Dep. Variable:			GI_SST	No. Observations:		420
Model:	SARIMAX(1, 1, 1)x(0, 1, 1, 12)			Log Likelihood		-147.221
Date:		Mon, 08 Nov 2021		AIC		304.441
Time:			19:41:04	BIC		324.310
Sample:			01-31-1986	HQIC		312.315
			- 12-31-2020			
Covariance Type:			opg			

	coef	std err	z	P>|z|	[0.025	0.975]
intercept	-1.58e-07	0.000	-0.001	0.999	-0.000	0.000
ar.L1	0.3625	0.053	6.866	0.000	0.259	0.466
ma.L1	-1.0583	0.029	-36.622	0.000	-1.115	-1.002
ma.S.L12	-0.9719	0.068	-14.292	0.000	-1.105	-0.839
sigma2	0.1035	0.010	9.940	0.000	0.083	0.124

Ljung-Box (L1) (Q):	0.01	Jarque-Bera (JB):	1.27
Prob(Q):	0.92	Prob(JB):	0.53
Heteroskedasticity (H):	0.74	Skew:	-0.14
Prob(H) (two-sided):	0.09	Kurtosis:	3.06

Equation 12

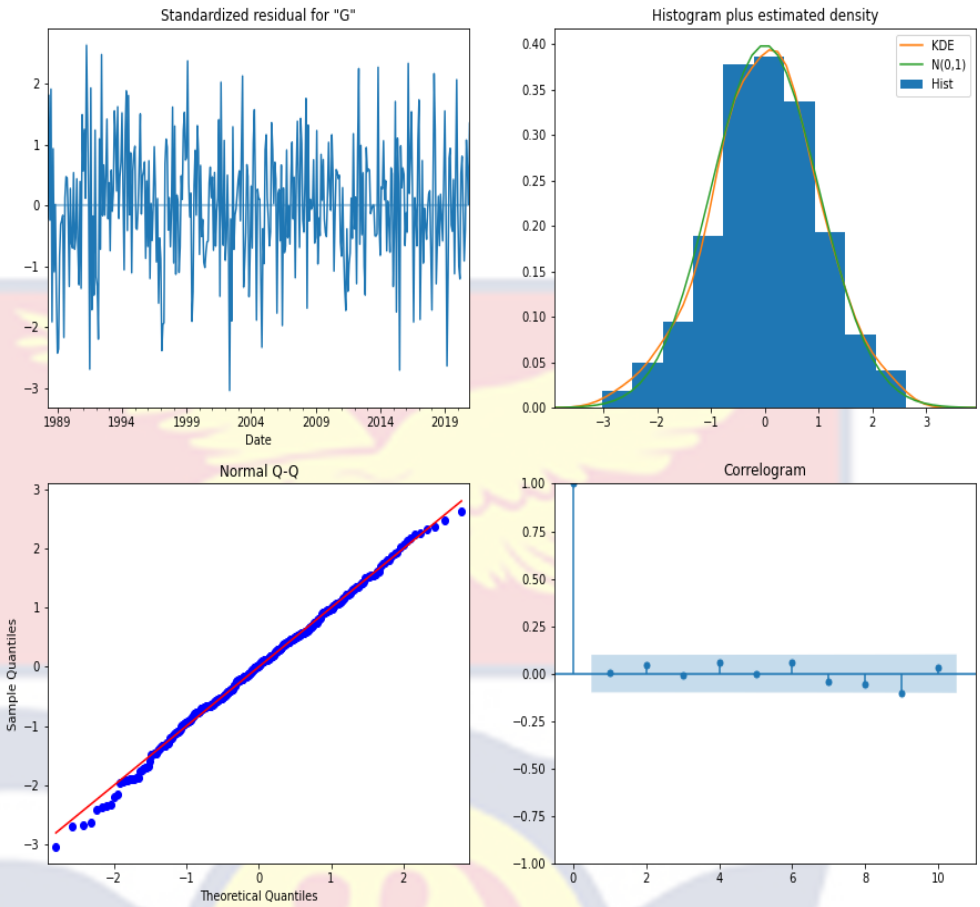

Figure 15: SARIMA residual plots

The normal quantile (Q-Q) plot and histogram in Figure 16 show that the error term follows a normal distribution. Furthermore, the correlogram shows that there is no autocorrelation in the error term. This indicates that the fitted model is appropriate.

The forecast for the next 10 years using the fitted model is presented in Figure 17 (a). Furthermore, Figure 17 (b) illustrates that in the next 10 years, the temperature for the hottest months is expected to increase in the region.

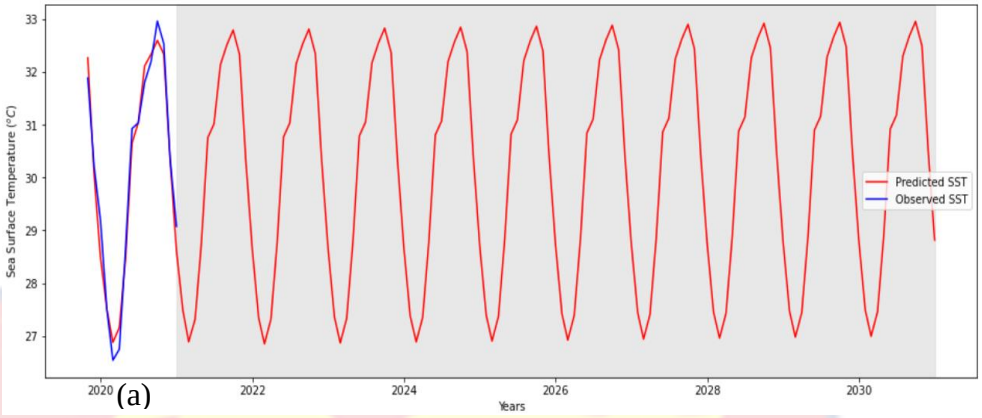

(a)

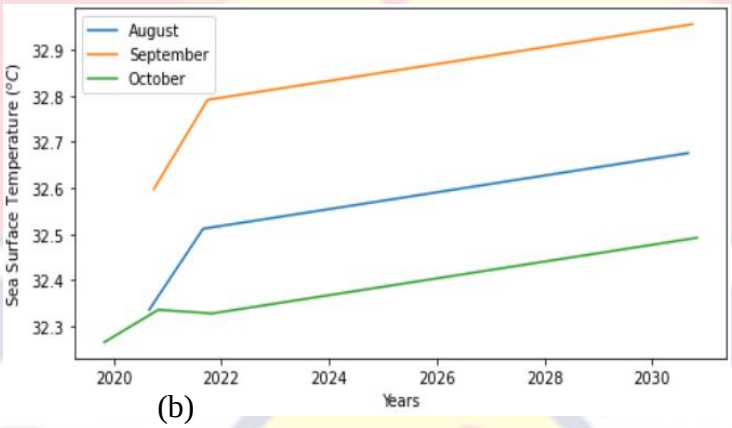

(b)

Figure: (a). Sea surface temperature forecast for the next 10 years, (b). Sea surface temperature forecast for the hottest months.

The Shapiro test p-values for the normality of SST data are all less than (Sheik Seid Island, 0.010; Gurgusum, 0.011; Durgella, 0.014). As a result, the SST data's normality assumption is violated and hence was transformed using the Box-Cox transformation method to overcome this assumption violation, resulting in a normally distributed data. Furthermore, Leven's test was used to assess variance equality across the three sites, and it was found to be non-significant for all three datasets: yearly average SST, yearly average SSTA, and yearly average DHW.

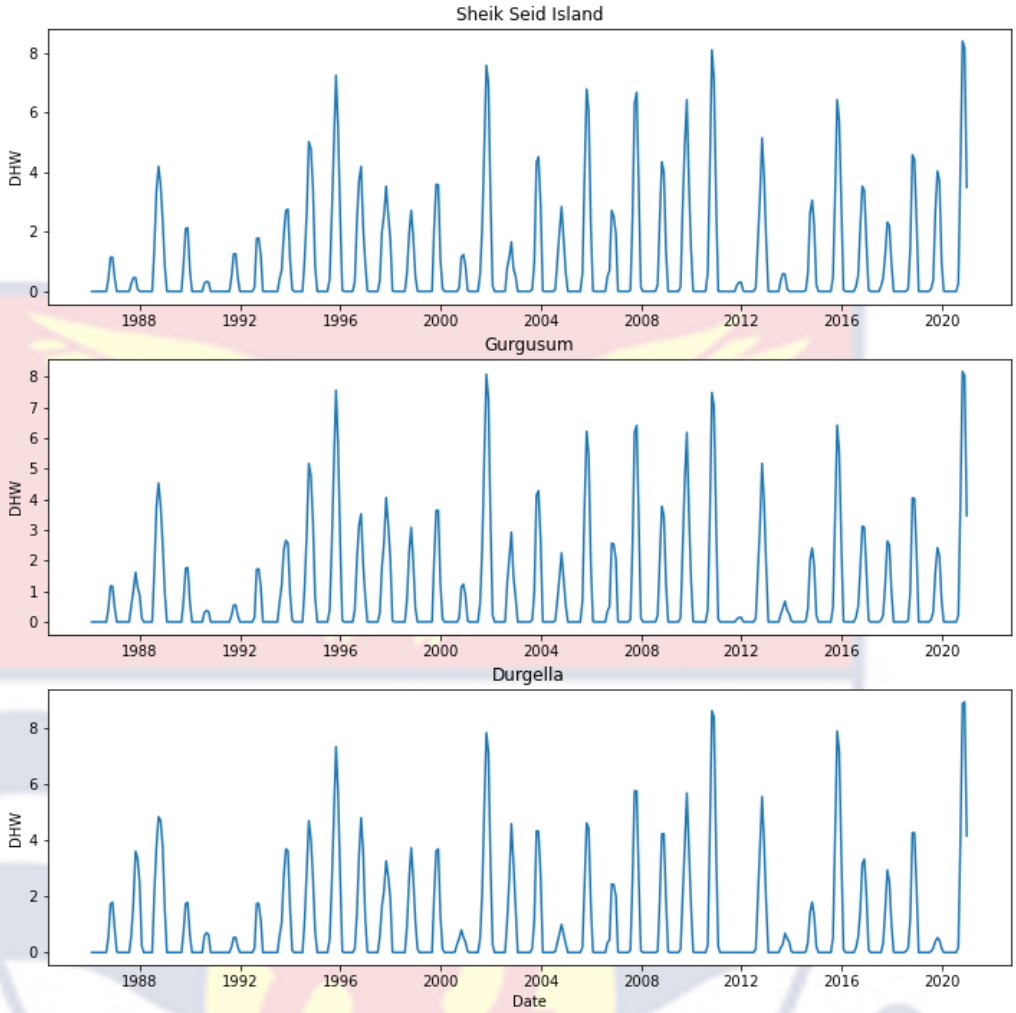

Figure 16: Yearly degree heat week occurrences within the selected sites.

An ANOVA test result showed that there was a statistically significant difference (p-value < 0.05) in SST among the Sites. Furthermore, Table 5 provides the Tukey post hoc test results which shows a statistically significant difference between all the pairs of sites (p-value < 0.05). On the other hand, no statistical difference (p-value > 0.05) among sites was observed for SSTA and DHW data.

Table 5: P-values for post hoc-Tukey test for comparison of SST among sites (p-value≤0.05 indicates significant difference).

	Sheik Seid Island	Gurgusum	Durgella
Sheik Seid Island	1.000	0.001	0.001
Gurgusum	0.001	1.000	0.028
Durgella Island	0.001	0.028	1.000

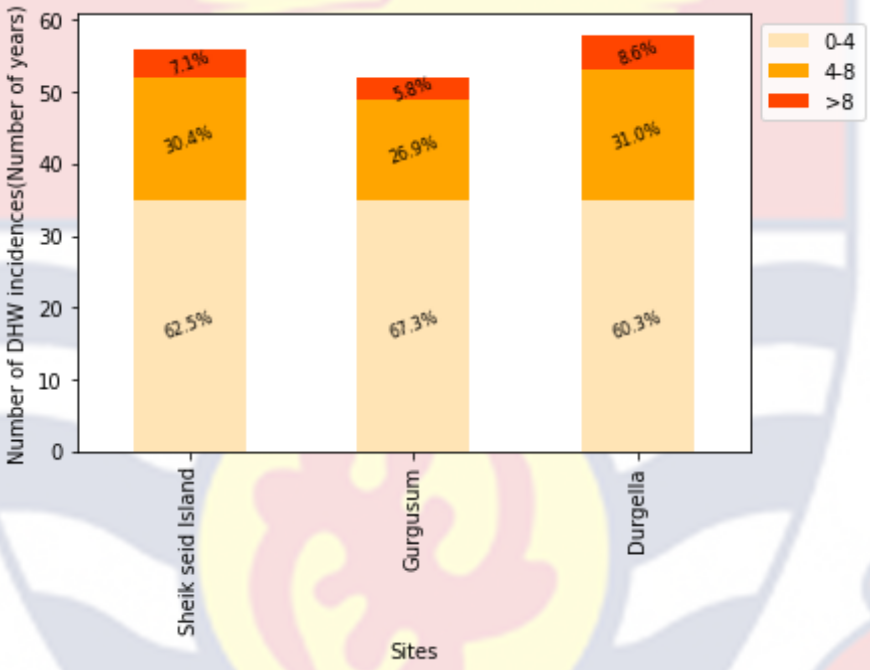

Figure 17: Temperature at 0, 4, and 8°C-weeks that demonstrates DHW severity.

Figure 18 shows, more than 4°C-weeks of DHW is always associated with widespread bleaching, and more than 8°C-weeks is always associated with widespread mortality. To quantify the intensity of DHWs, maximum DHWs values were classified into three groups: 0-4, 4-8, and >8°C weeks for each site, and plotted in a stacked bar plot. The bar plot depicts the high intensity of DHWs > 8°C weeks at Durgella, an Eritrean Red Sea site.

Figure 18: Degree heat weeks (DHW) in three sites on the southern part of the Red Sea during the years 1986-2020.

Figure 19 portrays a scatterplot of the annual maximum DHW occurrences in the years 1986-2020. The three sides are represented using different colors while the size of the circle (scatter point) illustrates the magnitude of the DHW. The fitted lines show that there is an increase of annual maximum DHW in all the sites.

SST and Chlorophyll-a

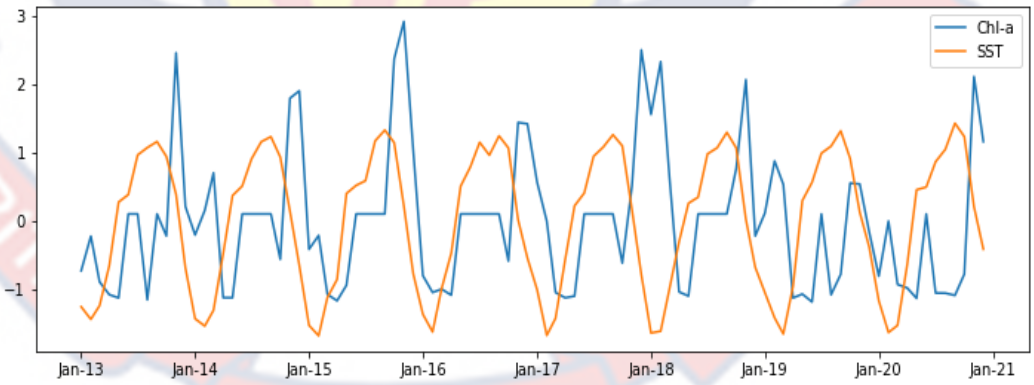

Figure 19: Chlorophyll-a and SST time series data of study area. The data were standardized in order to have the same scale.

To get a better insight of the seasonality of SST and chlorophyll-a, they are both plotted in one plot given in Figure 20. Both datasets were

standardized to have the same scale. In general, chlorophyll-a appears to be increasing when SST decreases and, in some months, also they are increasing at the same time.

Coral coverage

Figure 20 shows the coverage of different benthic communities in the three sites under consideration through the years 2013-2020. Gurgusum has the least live coral coverage and the highest rubble coverage compared to the other sites. Moreover, the live coral coverage appears to be decreasing in all the sites.

Figure 20: Coverage of different components over the years 2013-2020.

The multivariate analysis of variance (MANOVA) result given in Table 6, shows that there is a significant coverage difference among sites (p-value for Wilks' lambda < 0.05). However, no significant difference is observed between the years (p-value >0.05). Thus, for further investigation in the coverage difference among sites for the different components, a one-way ANOVA tests were conducted.

Table 6: MANOVA output: Comparison of coverage of the components among Sites and Years.

Multivariate linear model

Intercept	Value	Num DF	Den DF	F Value	Pr > F
Wilks' lambda	0.0006	6.0000	9.0000	2477.4619	0.0000
Pillai's trace	0.9994	6.0000	9.0000	2477.4619	0.0000
Hotelling-Lawley trace	1651.6413	6.0000	9.0000	2477.4619	0.0000
Roy's greatest root	1651.6413	6.0000	9.0000	2477.4619	0.0000

Sites	Value	Num DF	Den DF	F Value	Pr > F
Wilks' lambda	0.0015	12.0000	18.0000	36.7794	0.0000
Pillai's trace	1.8467	12.0000	20.0000	20.0836	0.0000
Hotelling-Lawley trace	97.8073	12.0000	11.2727	69.3601	0.0000
Roy's greatest root	91.7886	6.0000	10.0000	152.9810	0.0000

Years	Value	Num DF	Den DF	F Value	Pr > F
Wilks' lambda	0.0421	42.0000	45.6658	1.0490	0.4358
Pillai's trace	1.8881	42.0000	84.0000	0.9183	0.6126
Hotelling-Lawley trace	6.6099	42.0000	16.3944	1.2547	0.3171
Roy's greatest root	4.3725	7.0000	14.0000	8.7449	0.0003

In multivariate analysis of variance, it is important to note that to conduct an individual one-way ANOVA, the significance level to be used is $\frac{\alpha}{c}$, where c, is the number of independent variables and α is the significance

level used for the MANOVA test. In this case, since there are six independent variables (Coral loss, Live coral, Rubble, Sponge, Turf algae, Crustose coralline algae), the significance level to be used for each of the individual one-way ANOVAs is $\frac{0.05}{6} = 0.0083$. Based on this significance level, Tables 7-10 show that there exists a statistically significant difference in coverage among the three sites for Live coral, Rubble, Sponge, and crustose coralline algae.

Table 7 shows that the percentage of live coral coverage differs significantly (p-value < 0.05) between Sheik Seid Island and Gurgusum. However, the other pair of comparison did not show statistically significant differences (p-value > 0.05).

Table 7: Tukey HSD pairwise comparison for Live coral coverage.

Multiple Comparison of Means - Tukey HSD, FWER=0.01

group1	group2	meandiff	p-adj	lower	upper	reject
Durgella	Gurgusum	6.6418	0.3677	-9.7097	22.9934	False
Durgella	Sheik Seid Island	-10.9636	0.0801	-27.3152	5.3879	False
Gurgusum	Sheik Seid Island	-17.6054	0.0039	-33.957	-1.2539	True

The Tukey HSD pairwise comparison provided in Table 8, shows that rubble coverage in Gurgusum is significantly different (p-value < 0.05) from the other two sites. However, no statistically significant difference (p-value > 0.05) of rubble coverage was observed between Durgella and Sheik Seid Island.

Table 8: Tukey HSD pairwise comparison for Rubble coverage.

Multiple Comparison of Means - Tukey HSD, FWER=0.01

group1	group2	meandiff	p-adj	lower	upper	reject
Durgella	Gurgusum	4.6542	0.001	1.5994	7.709	True
Durgella	Sheik Seid Island	0.3273	0.9	-2.7275	3.3821	False
Gurgusum	Sheik Seid Island	-4.327	0.001	-7.3818	-1.2721	True

Table 9 shows that the sponge coverage in Gurgusum is significantly different from that of Durgella (p-value < 0.05). The sponges are mostly located in Durgella than the others and few are covered in sheik seid.

Table 9: Tukey HSD pairwise comparison for Sponge coverage.

Multiple Comparison of Means - Tukey HSD, FWER=0.01

group1	group2	meandiff	p-adj	lower	upper	reject
Durgella	Gurgusum	-0.2912	0.001	-0.4784	-0.1041	True
Durgella	Sheik Seid Island	-0.14	0.047	-0.3271	0.0471	False
Gurgusum	Sheik Seid Island	0.1512	0.0305	-0.0359	0.3384	False

Table 10 shows that the crustose coralline algae coverage in Gurgusum is significantly different from that in Durgella (p-value < 0.05).

Table 10: Tukey HSD pairwise comparison for crustose coralline algae coverage.

Multiple Comparison of Means - Tukey HSD, FWER=0.01

group1	group2	meandiff	p-adj	lower	upper	reject
Durgella	Gurgusum	-0.2912	0.001	-0.4784	-0.1041	True
Durgella	Sheik Seid Island	-0.14	0.047	-0.3271	0.0471	False
Gurgusum	Sheik Seid Island	0.1512	0.0305	-0.0359	0.3384	False

Table 10 shows that algae coverage around Durgella was observed to be significantly lower than that of Gurgusum. However, no significant difference of algae coverage was observed between Sheik Seid Island and the other two sites.

CHAPTER FIVE

DISCUSSION

Supervised Classification

Classification accuracy and misclassification errors of three image classifiers: Support vector machines (SVM), maximum likelihood classifier (MLC), and random forest classifier, was compared using an atmospherically corrected image. Overall, SVM produced the most accurate results compared to the other two models. On the other hand, maximum likelihood classifier produced the lowest classification accuracy, which can be assigned to its assumption of normal class distribution, which is an infrequent occurrence for sample classes. The image classifications produced a five-class benthic map (Coral, Mangroves, Sand, Rubbles, and a combination of coral, rubbles, sands, and algae) that shows the distribution of each of these five classes.

The SVM classifier, with an accuracy of 73.4%, produced the most accurate classification results (Table 2). After atmospheric correction of satellite imagery, user accuracy of live corals increased to 89.47% (Figure 11 (ii)). Once again, coral habitats were misidentified as a mix of coral/sand/algae and rubble habitats. When classifications (i) and (ii) are compared to classification (iii), the depth restriction of live corals in both (i) and (ii) lacks sharp distinction, whereas in (iii), live corals have clearer seaward boundaries. The SVM-derived habitat map of bottom reflectance (Figure 11 – iii) was determined to be the most accurate of the three habitat maps at the Massawa survey site after a quantitative and qualitative examination of the classified habitat maps.

Sea surface temperature, anomality and Degree heat week (DHW) on coral reef

Hydrographic conditions in the Red Sea water vary from location to location. As such, most research on hydrographic parameters differs through the various geographical zones namely the northern, central, and southern parts) of the Red Sea. In essence, the science of the Red Sea differs from one zonation to the other. Chapter two mentions that the Red Sea is a semi-enclosed water body that stretches from the north Suez Canal to south Bab-El-Mandeb (Gulf of Aden). Most studies have discussed the water flow and other physical processes affecting the reefs' decline (Hughes & Connell, 1999).

Figure 13 shows that the SST data for all sites appear to be trending upward. Based on the Mann-Kendall test results, there was a significant increase in sea SST from 1986 to 2020. This is in line with projected rise (1–2°C) reported by the IPCC for tropical oceans and is expected to progressively create hostile conditions for coral reefs as reported by Brown (1997).

The difference in DWH and SSTA among the three study sites was found to be non-significant. For SST, however, a significant difference was observed among the three study sites under consideration. Furthermore, a Tukey pair-wise test showed that the average monthly SST of each site is significantly different than the others. A prediction for the next ten years using a seasonal ARIMA model showed that SST will be trending up. From Table 3 it is observed that the SST increase around Sheik Seid Island is higher.

Overall, the SARIMA model results for the next ten years show an increasing trend in sea surface temperature from 0.2-0.9°C around the selected sites. Furthermore, if SST continues to rise in the coming years, the coral reef

ecosystem will suffer greatly as it was evident during the El Niño 2015/2016 which resulted in higher depletion of the Gurgusum reef (Kasimala et al., 2020).

Furthermore, if the SST continues to increase, the services provided by the coral reef ecosystem will have a massive impact on Eritrea's livelihood and coastal area. The temperature threshold limit is not an absolute value; there are reefs with high or warm sea surface temperatures, for example, most literatures mention coral reefs in the northern Red Sea as thermally tolerant reefs. The southern red sea experiences high mixing of water from the Indian Ocean through the Gulf of Aden toward the southern red sea, causing high stresses to ecosystems and resulting in high sea surface temperature fluctuations over the last 34 years. If the DHWs value is less than 8^{o}C and no additional human stressors are present, corals have a natural ability to recover from bleaching. To implement successful ecosystem conservation, stakeholders should collaborate on conservation management and policy formation for monitoring of the ecosystems.

The statistical comparison tests show that the three sites have significant differences in terms of the coverage of live coral, coral loss, Rubble, and Sponge. This result combined with graph in Figure 20 shows that there is a higher rate of coral loss around Sheik Seid Island. In addition, it was observed that there is significantly higher live coral coverage in Durgella island compared.

The Sheik Seid Island has more anthropogenic activity than others due to its popularity as a tourist destination, its closeness to the city, and the amount of effluent and water mixing from the power plant. Gurgusum is also

in Massawa, close to the cement factory with less human activities. Durgella island is far from the above sites, with few anthropogenic activities such as anchoring artisanal fishing boats.

Sea surface temperature and Chlorophyll – a

Most studies on primary productivity around the red sea water bodies report that winds and Chl-a have significant correlations due to the flowing water currents from the Gulf of Aden. According to Patzert (1974), the red sea water bodies are divided into two sections of wind flow. The northwest wind drives the northern part of the red sea during the whole year. Still, in the southern part of the red sea, the movement of the water bodies is controlled by two different winds over the entire year, the southwest wind flows from the south during the winter, and during the summer, the northern west wind flows from the north. Figure 18 shows an increase in SST and Chl-a during the summer season, which the impact of northwest wind can explain, which drives upwelling in the region at that time (Elawad, 2012).

The negative correlation between Chlorophyll-a and temperature (-0.47) shows that there was different behavior in the water; as discussed above, there is a highly significant relationship between wind and Chl-a in the southern part of the red sea. As a result, the correlation between the Chl-a and SST is consistent and shows it affected the growth of the reef. Figure 19 indicates the maximum annual sea surface temperature in reef thermal limits in the study sites. SST determined to have an effect on Chl-a, Figure 13, was consistently high during the summer from June to October reaching a high value of 35℃ in September, and decreased during winter until it reaches a minimum level of 26℃ in February.

Chl-a dynamics always starts with the beginning of winter. However, in this area, the blooms begin in September and end in February with a maximum occurrence of 5.5 mg/m^3) in December, and the concentration goes down until the end of bloom (Figure 21).

During the hot summer season, the study area exhibits comparatively high productivity as shown in Figure 21. Currently, the Northwest monsoon winds sail the hot, saline northern surface Red Sea waters from north to south and this results in the southern Red Sea surface water to be hotter. At the same time this area shows high productivity due to the entrance of the nutrient loaded Gulf of Aden Intermediate Water (GAIW) provoked by Northwest winds during this season.

The present paradigm in tropical waters like in the southern Red Sea is that SST and Chl-a are negatively correlated. Warm waters are expected to be less productive as stated by Behrenfeld et al. (2006) and Doney (2006) and the waters are ventilated by convective vertical overturning processes. The result of upwelling is the influx of nutrient loaded, deeper and colder water to the surface, which causes SST of the area to decrease. This, in turn, increases productivity of the environment. Therefore, hot waters are associated with less productive areas. Although the southern Red Sea is expected to have higher thermal stratification during the hot season (summer), the unique characteristic of the area causes a positive relationship between SST and Chl-a unlike the in counterpart tropical waters. This is because, the southern Red Sea depends on wind induced horizontal currents for their nutrient nourishment rather than vertical convective overturning processes (Raitsos et al., 2015) and thus the

horizontal wind movements are significantly strong enough to bring nutrient rich water from the Indian Ocean (Dreano et al., 2016).

The correlation between Chl-a and SST is positive in the summer but negative in the autumn, winter, and spring. During the winter, the Southeast monsoon winds bring in relatively colder Gulf of Aden surface water, making the southern Red Sea productive but colder, causing the two variables to be negatively correlated.

CHAPTER SIX

CONCLUSION AND RECOMMENDATION

Conclusions

In this study, the classification accuracy of three image classifiers - Support Vector Machines (SVM), Maximum Likelihood Classifier (MLC), and Random Forest Classifier - were evaluated using an atmospherically corrected image. The results indicated that SVM outperformed the other two models in terms of accuracy. On the other hand, MLC exhibited the lowest classification accuracy due to its assumption of normal class distribution, which was not frequently observed in the sample classes.

Again, SST differences among the study sites were found to be significant, with Sheik Seid Island showing the highest increase. A seasonal ARIMA model predicted a continued upward trend in SST over the next decade, potentially affecting the coral reef ecosystem and livelihoods in Eritrea's coastal areas. Statistical comparisons and observations indicated higher rates of coral loss around Sheik Seid Island, attributed to its popularity as a tourist destination and proximity to human activities such as a power plant. Similarly, Durgella Island had relatively higher live coral coverage, while Gurgusum faced fewer anthropogenic activities near the cement factory in Massawa.

Furthermore, the study also showed that during the summer season, there is an increase in sea surface temperature (SST) and Chl-a, attributed to the impact of the northwest wind causing upwelling. The negative correlation between Chl-a and temperature (-0.47) indicates different water behavior, with a significant relationship between wind and Chl-a in the southern Red Sea.

SST has an effect on Chl-a dynamics, with high temperatures observed during summer and lower temperatures during winter. Chl-a blooms typically begin in September and end in February, reaching a maximum concentration in December. The southern Red Sea exhibits high productivity during the hot summer season due to the nutrient-loaded Gulf of Aden Intermediate Water brought by the Northwest winds.

Contrary to the paradigm in tropical waters, where warm waters are expected to be less productive, the southern Red Sea shows a positive correlation between SST and Chl-a. This is because the area relies on wind-induced horizontal currents for nutrient nourishment rather than vertical convective overturning processes. The strong horizontal wind movements bring nutrient-rich water from the Indian Ocean. The correlation between Chl-a and SST is positive in summer but negative in autumn, winter, and spring. During winter, the Southeast monsoon winds bring in colder Gulf of Aden surface water, making the southern Red Sea productive but colder, leading to the negative correlation between the two variables.

Chlorophyll-a concentration is an indicator of the amount of phytoplankton present in the water. When the concentration of chlorophyll-a is high, it indicates an increase in the number of phytoplankton which, in turn, can absorb more sunlight and warm up the surface waters. This warming can then add to the stress on corals caused by rising sea surface temperatures. The combination of high seawater temperatures and increased levels of chlorophyll-a can make it very difficult for coral to recover from bleaching events. Additionally, high levels of chlorophyll-a can indicate that there is an

excess of nutrients in the water which can promote the growth of harmful algae that can harm the coral even further.

Policy Recommendations

Based on the findings regarding hydrographic conditions and primary productivity in the Red Sea, the following policy recommendation is proposed:

Integrated Monitoring and Management Approach: Implement an integrated monitoring and management approach for the Red Sea that considers the variations in hydrographic conditions and primary productivity across different regions. This approach should involve collaboration among stakeholders, including government agencies, research institutions, and local communities.

Strengthen Research Efforts: Allocate resources and support research initiatives focused on understanding the complex relationships between hydrographic parameters, primary productivity, and the impacts on coral reef ecosystems. Encourage interdisciplinary studies to capture the interactions between physical processes, nutrient dynamics, and biological responses.

Climate Change Mitigation: Develop and implement measures to mitigate the effects of climate change on the Red Sea. This includes reducing greenhouse gas emissions, promoting renewable energy sources, and supporting initiatives that address climate change adaptation and resilience.

Sustainable Tourism and Coastal Development: Encourage sustainable tourism practices and responsible coastal development to minimize anthropogenic impacts on the Red Sea. Implement regulations and guidelines for tourism

operators, ensuring sustainable practices that minimize pollution, habitat destruction, and disturbance to marine ecosystems.

Conservation and Restoration Efforts: Support initiatives for the conservation and restoration of coral reefs in the Red Sea. This can include the establishment of marine protected areas, implementation of coral reef restoration projects, and promoting community engagement in conservation efforts.

Capacity Building and Public Awareness: Invest in capacity building programs and public awareness campaigns to enhance understanding of the importance of the Red Sea's hydrographic conditions and primary productivity. Educate local communities, stakeholders, and policymakers about the significance of preserving marine ecosystems and the potential consequences of environmental degradation.

International Cooperation: Foster international cooperation and collaboration among Red Sea countries to address transboundary issues and develop shared strategies for the sustainable management of the Red Sea's resources. This can involve joint research projects, information sharing, and the establishment of cooperative frameworks.

By implementing these policy recommendations, it is possible to enhance the understanding of the Red Sea's hydrographic conditions, protect its biodiversity, and promote sustainable development practices for the benefit of current and future generations.

REFERENCES

Alliance, C. R. (2003). Watersheds and Healthy Reefs: Making the Connection. The Coral Reef Alliance, San Francisco, United States.

Alliance, C. (2006). Coral Reefs and Sustainable Marine Recreation.

Ampou, E. E., Johan, O., Menkès, C. E., Niño, F., Birol, F., Ouillon, S., & Andréfouët, S. (2017). Coral mortality induced by the 2015–2016 El-Niño in Indonesia: the effect of rapid sea level fall. Biogeosciences, 14(4), 817-826.

Ateweberhan, M. (2004). Seasonal dynamics of coral reef algae in the southern Red Sea: functional group and population ecology.

Baker, A. C., Glynn, P. W., & Riegl, B. (2008). Climate change and coral reef bleaching: An ecological assessment of long-term impacts, recovery trends and future outlook. Estuarine, coastal and shelf science, 80(4), 435-471.

Baswapoor, S., & Irfan, Z. B. (2018). Current status of coral reefs in India: importance, rising threats and policies for its conservation and management (No. 2016-175).

Beenaerts, N., & Berghe, E. V. (2005). Comparative study of three transect methods to assess coral cover, richness and diversity. Western Indian Ocean Journal of Marine Science, 4(1), 29-38.

Behairy, A. K. A., Rao, N. D., & El-Shater, A. (1991). A siliciclastic coastal sabkha, Red Sea coast, Saudi Arabia. Marine Scienes, 2(1).

Behrenfeld, M. J., O'Malley, R. T., Siegel, D. A., McClain, C. R., Sarmiento, J. L., Feldman, G. C., ... & Boss, E. S. (2006). Climate-driven trends in contemporary ocean productivity. Nature, 444(7120), 752-755.

Bellwood, D. R., & Wainwright, P. C. (2002). The history and biogeography of fishes on coral reefs. Coral reef fishes: dynamics and diversity in a complex ecosystem, 5, 32.

Bellwood, D. R., Hughes, T. P., Folke, C., & Nyström, M. (2004). Confronting the coral reef crisis. Nature, 429(6994), 827-833.

Ben-Avraham, Z., & Grasso, M. (1991). Crustal structure variations and transcurrent faulting at the eastern and western margins of the eastern Mediterranean. Tectonophysics, 196(3-4), 269-277.

Berkelmans, R. (2002). Time-integrated thermal bleaching thresholds of reefs and their variation on the Great Barrier Reef. Marine ecology progress series, 229, 73-82.

Berumen, M. L., Hoey, A. S., Bass, W. H., Bouwmeester, J., Catania, D., Cochran, J. E. M., ... & Saenz-Agudelo, P. (2013). The status of coral reef ecology research in the Red Sea. *Coral Reefs*, *32*(3), 737-748.

Booth, D. J., & Beretta, G. A. (2002). Changes in a fish assemblage after a coral bleaching event. Marine Ecology Progress Series, 245, 205-212.

Bosworth, W. (2015). Geological evolution of the Red Sea: historical background, review, and synthesis. In The Red Sea (pp. 45-78). Springer, Berlin, Heidelberg.

Breiman, L. (2001). Random forests. Machine learning, 45, 5-32.

Brown, B. E. (1997). Coral bleaching: causes and consequences. Coral reefs, 16, S129-S138.

Burke, L., Reytar, K., Spalding, M., & Perry, A. (2011). Reefs at risk revisited. World Resources Institute.

Burkepile, D. E., & Hay, M. E. (2008). Coral Reefs. In S. E. Jørgensen, & B. D. Fath, Encyclopedia of Ecology (pp. 784-796). Academic Press.

Cantin, N. E., & Lough, J. M. (2014). Surviving coral bleaching events: Porites growth anomalies on the Great Barrier Reef. PloS one, 9(2), e88720.

Chaidez, V., Dreano, D., Agusti, S., Duarte, C. M., & Hoteit, I. (2017). Decadal trends in Red Sea maximum surface temperature. Scientific reports, 7(1), 1-8.

Chong-Seng, K. M., Mannering, T. D., Pratchett, M. S., Bellwood, D. R., & Graham, N. A. (2012). The influence of coral reef benthic condition on associated fish assemblages.

Cochran, J. R. (1983). A model for development of Red Sea. Aapg Bulletin, 67(1), 41-69.

Cochran, J. R., & Karner, G. D. (2007). Constraints on the deformation and rupturing of continental lithosphere of the Red Sea: the transition from rifting to drifting. Geological Society, London, Special Publications, 282(1), 265-289.

Coleman, R. G. (1974). Geologic background of the Red Sea. In The geology of continental margins (pp. 743-751). Springer, Berlin, Heidelberg.

Coles, S. L., & Jokiel, P. L. (1978). Synergistic effects of temperature, salinity and light on the hermatypic coral Montipora verrucosa. Marine Biology, 49, 187-195.

Congalton, R. G. (1991). A review of assessing the accuracy of classifications of remotely sensed data. Remote sensing of environment, 37(1), 35-46.

Cornillon, P., Stramma, L., & Price, J. F. (1987). Satellite measurements of sea surface cooling during hurricane Gloria. Nature, 326(6111), 373-375.

Courtillot, V., Jaupart, C., Manighetti, I., Tapponnier, P., & Besse, J. (1999). On causal links between flood basalts and continental breakup. Earth and Planetary Science Letters, 166(3-4), 177-195.

De Grissac, A. J., & Negussie, N. (2007). Government of Eritrea and UNDP. Eritrea's coastal marine and island biodiversity conservation project.

dei Lincei, A. N. (1980). Geodynamic Evolution of the Afro-Arabian Rift System. Rome, Accademia Nazionale dei Lincei («Atti Convegni Lincei», 47), 65-73.

DeVantier, L., Turak, E., Al-Shaikh, K., & De ath, G. (2000). Coral communities of the central-northern Saudi Arabian Red Sea. Fauna of Arabia, 18, 23-66.

Dewi, C. S. U., Capriati, A., Prabuning, D., Maududi, A., & Harsindhi, C. J. (2021, April). Current status of coral reef ecosystems in Brumbun Bay, Tulungagung. In IOP Conference Series: Earth and Environmental Science (Vol. 744, No. 1, p. 012082). IOP Publishing.

DiBattista, J. D., Howard Choat, J., Gaither, M. R., Hobbs, J. P. A., Lozano-Cortés, D. F., Myers, R. F., ... & Berumen, M. L. (2016). On the origin of endemic species in the Red Sea. Journal of Biogeography, 43(1), 13-30.

Doney, S. C. (2006). Plankton in a warmer world. Nature, 444(7120), 695-696.

Donovan, M. K., Friedlander, A. M., Lecky, J., Jouffray, J. B., Williams, G. J., Wedding, L. M., ... & Selkoe, K. A. (2018). Combining fish and benthic communities into multiple regimes reveals complex reef dynamics. Scientific reports, 8(1), 1-11.

Dreano, D., Raitsos, D. E., Gittings, J., Krokos, G., & Hoteit, I. (2016). The Gulf of Aden intermediate water intrusion regulates the southern Red Sea summer phytoplankton blooms. PloS one, 11(12), e0168440.

Edwards, R. L., Chen, J. H., & Wasserburg, G. J. (1987). 238U234U230Th2 32Th systematics and the precise measurement of time over the past 500,000 years. Earth and Planetary Science Letters, 81(2-3), 175-192.

Elawad, A. E. S. (2012). Study of inter-annual variability of chlorophyll in the Red Sea (Master's thesis, The University of Bergen).

Evans, S. D. (1997). The green republic: a conservation history of Costa Rica, 1838-1996. University of Kansas.

Fautin, D. G., & Buddemeier, R. W. (1993). Coral bleaching as an adaptive mechanism: a testable hypothesis. Bioscience, 45, 320-326.

Foo, S. A., & Asner, G. P. (2019). Scaling up coral reef restoration using remote sensing technology. Frontiers in Marine Science, 79.

Gass, I. G. (1970). The evolution of volcanism in the junction area of the Red Sea, Gulf of Aden and Ethiopian rifts. Philosophical Transactions for the Royal Society of London. Series A, Mathematical and Physical Sciences, 369-381.

Gibson, R., & Sundberg, P. (2001). Some nemerteans (Nemertea) from Queensland and the Great Barrier Reef, Australia. Zoological science, 18(9), 1259-1273.

Gillespie, J. (2020). Protected Areas: A Legal Geography Approach. Springer Nature.

Girdler, R. W., & Southren, T. C. (1987). Structure and evolution of the northern Red Sea. Nature, 330(6150), 716-721.

Gislason, P. O., Benediktsson, J. A., & Sveinsson, J. R. (2006). Random forests for land cover classification. Pattern recognition letters, 27(4), 294-300.

Glynn, P. W., & D'croz, L. (1990). Experimental evidence for high temperature stress as the cause of El Niño-coincident coral mortality. Coral reefs, 8, 181-191.

Glynn, P. W. (1993). Coral reef bleaching: ecological perspectives. Coral reefs, 12(1), 1-17.

Glynn, P. W. (1996). Coral reef bleaching: facts, hypotheses and implications. Global change biology, 2(6), 495-509.

Glynn, P. W., Mones, A. B., Podestá, G. P., Colbert, A., & Colgan, M. W. (2017). El Niño-Southern Oscillation: effects on Eastern Pacific coral reefs and associated biota. In Coral reefs of the eastern tropical Pacific (pp. 251-290). Springer, Dordrecht.

Goldberg, J., & Wilkinson, C. (2004). Global threats to coral reefs: coral bleaching, global climate change, disease, predator plagues and invasive species. Status of coral reefs of the world, 2004, 67-92.

Goreau, T. J., & Macfarlane, A. H. (1990). Reduced growth rate of Montastrea annularis following the 1987–1988 coral-bleaching event. Coral Reefs, 8(4), 211-215.

Goudie, A. S., & Middleton, N. J. (2006). Desert dust in the global system. Springer Science & Business Media.

Gove, J. M., Williams, G. J., McManus, M. A., Heron, S. F., Sandin, S. A., Vetter, O. J., & Foley, D. G. (2013). Quantifying climatological ranges and anomalies for Pacific coral reef ecosystems. PloS one, 8(4), e61974.

Graham, N. A. J., & Nash, K. L. (2013). The importance of structural complexity in coral reef ecosystems. Coral reefs, 32(2), 315-326.

Gray, J. S., & Mirza, F. B. (1979). A possible method for the detection of pollution-induced disturbance on marine benthic communities. Marine Pollution Bulletin, 10(5), 142-146.

Greer, L., Jackson, J. E., Curran, H. A., Guilderson, T., & Teneva, L. (2009). How vulnerable is Acropora cervicornis to environmental change? Lessons from the early to middle Holocene. Geology, 37(3), 263-266.

Halford, J. C., Gillespie, J., Brown, V., Pontin, E. E., & Dovey, T. M. (2004). Effect of television advertisements for foods on food consumption in children. Appetite, 42(2), 221-225.

Harborne, A. R., Rogers, A., Bozec, Y. M., & Mumby, P. J. (2017). Multiple stressors and the functioning of coral reefs. Annual Review of Marine Science, 9, 445-468.

Hedberg, N., Kautsky, N., Hellström, M., & Tedengren, M. (2015). Spatial correlation and potential conflicts between sea cage farms and coral reefs in Southeast Asia. Aquaculture, 448, 418-426.

Heenan, A., Hoey, A. S., Williams, G. J., & Williams, I. D. (2016). Natural bounds on herbivorous coral reef fishes. Proceedings of the Royal Society B: Biological Sciences, 283(1843), 20161716.

Hicks, C. C., & Cinner, J. E. (2014). Social, institutional, and knowledge mechanisms mediate diverse ecosystem service benefits from coral reefs. Proceedings of the National Academy of Sciences, 111(50), 17791-17796.

Hillman, J., & Tsegay, S. (1997). Coral reef research and conservation in Eritrea: area profile. In Western Indian Ocean Regional Workshop on Coral Reef Research and Conservation, Mombasa.

Hughes, T. P., & Connell, J. H. (1999). Multiple stressors on coral reefs: A long-term perspective. Limnology and oceanography, 44(3part2), 932-940.

Hoegh-Guldberg, O. (1999). Climate change, coral bleaching and the future of the world's coral reefs. Marine and freshwater research, 50(8), 839-866.

Hoegh-Guldberg, O., Fine, M., Skirving, W., Johnstone, R., Dove, S., & Strong, A. (2005). Coral bleaching following wintry weather. Limnology and Oceanography, 50(1), 265-271.

Hoegh-Guldberg, O., Pendleton, L., & Kaup, A. (2019). People and the changing nature of coral reefs. Regional Studies in Marine Science, 30, 100699.

Hughes, K., Bellis, M. A., Hardcastle, K. A., Sethi, D., Butchart, A., Mikton, C., ... & Dunne, M. P. (2017). The effect of multiple adverse childhood experiences on health: a systematic review and meta-analysis. The Lancet Public Health, 2(8), e356-e366.

Hughes, L., Dwivedi, Y. K., Misra, S. K., Rana, N. P., Raghavan, V., & Akella, V. (2019). Blockchain research, practice and policy: Applications, benefits, limitations, emerging research themes and research agenda. International Journal of Information Management, 49, 114-129.

Hughes, T. P., Anderson, K. D., Connolly, S. R., Heron, S. F., Kerry, J. T., Lough, J. M., ... & Wilson, S. K. (2018). Spatial and temporal patterns of mass bleaching of corals in the Anthropocene. Science, 359(6371), 80-83.

Hughes, T. P., Baird, A. H., Bellwood, D. R., Card, M., Connolly, S. R., Folke, C., ... & Roughgarden, J. (2003). Climate change, human impacts, and the resilience of coral reefs. science, 301(5635), 929-933.

Hughes, T. P., Graham, N. A., Jackson, J. B., Mumby, P. J., & Steneck, R. S. (2010). Rising to the challenge of sustaining coral reef resilience. Trends in ecology & evolution, 25(11), 633-642.

Hughes, T. P., Rodrigues, M. J., Bellwood, D. R., Ceccarelli, D., Hoegh-Guldberg, O., McCook, L., ... & Willis, B. (2007). Phase shifts, herbivory, and the resilience of coral reefs to climate change. Current biology, 17(4), 360-365.

Jacques, T. G., Marshall, N., & Pilson, M. E. Q. (1983). Experimental ecology of the temperate scleractinian coral Astrangia danae: II. Effect of temperature, light intensity and symbiosis with zooxanthellae on metabolic rate and calcification. Marine Biology, 76, 135-148.

Jarrige, J. J., Ott d'Estevou, P., Burollet, P. F., Thiriet, J. P., Icart, J. C., Richert, J. P., ... & Prat, P. (1986). Inherited discontinuities and Neogene structure: the Gulf of Suez and the northwestern edge of the Red Sea. Philosophical Transactions of the Royal Society of London. Series A, Mathematical and Physical Sciences, 317(1539), 129-139.

Jeffrey, S. W., & Haxo, F. T. (1968). Photosynthetic pigments of symbiotic dinoflagellates (zooxanthellae) from corals and clams. The Biological Bulletin, 135(1), 149-165.

Joffe, S., & Garfunkel, Z. V. I. (1987). Plate kinematics of the circum Red Sea—a re-evaluation. Tectonophysics, 141(1-3), 5-22.

Jones, B., & Turki, A. (1997). Distribution and speciation of heavy metals in surficial sediments from the Tees Estuary, north-east England. Marine Pollution Bulletin, 34(10), 768-779.

Karner, S. L., Chester, F. M., Kronenberg, A. K., & Chester, J. S. (2003). Subcritical compaction and yielding of granular quartz sand. Tectonophysics, 377(3-4), 357-381.

Kasimala, M., Mogos, G. G., Negasi, K. T., Bereket, G. A., Abdu, M. M., & Melake, H. S. (2020). Biochemical composition of selected seaweeds from intertidal shallow waters of Southern Red Sea, Eritrea.

Khan, M.A. 1975. The Afro–Arabian rift system. Science Progress (1916), 62: 207–236.

Kotb, M. A., Hanafy, M. H., Rirache, H., Matsumura, S., Al-Sofyani, A. A., Ahmed, A. G., ... & Al-Horani, F. A. (2008). I n Status of Coral Reefs of the World: 2008. AIMS, Townsville, Australia.

Ladd, M. C., Miller, M. W., Hunt, J. H., Sharp, W. C., & Burkepile, D. E. (2018). Harnessing ecological processes to facilitate coral restoration. Frontiers in Ecology and the Environment, 16(4), 239-247.

Lazar, M., Ben-Avraham, Z., & Garfunkel, Z. (2012). The Red Sea–New insights from recent geophysical studies and the connection to the Dead Sea fault. Journal of African Earth Sciences, 68, 96-110.

Le Pichon, X., & Francheteau, J. (1978). A plate-tectonic analysis of the Red Sea—Gulf of Aden area. Tectonophysics, 46(3-4), 369-406.

Leigh Jr, E. G. (2010). The evolution of mutualism. Journal of evolutionary biology, 23(12), 2507-2528.

Lesser, M. P., Stochaj, W. R., Tapley, D. W., & Shick, J. M. (1990). Bleaching in coral reef anthozoans: effects of irradiance, ultraviolet radiation, and temperature on the activities of protective enzymes against active oxygen. Coral reefs, 8(4), 225-232.

Lin, B. (2021). Close encounters of the worst kind: reforms needed to curb coral reef damage by recreational divers. Coral Reefs, 40(5), 1429-1435.

Lirman, D., & Fong, P. (1997). Patterns of damage to the branching coral Acropora palmata following Hurricane Andrew: damage and survivorship of hurricane-generated asexual recruits. Journal of Coastal Research, 67-72.

Liu, G., Strong, A. E., & Skirving, W. (2003). Remote sensing of sea surface temperatures during 2002 Barrier Reef coral bleaching. Eos, Transactions American Geophysical Union, 84(15), 137-141.

Liu, G., Strong, A. E., Skirving, W., & Arzayus, L. F. (2006, June). Overview of NOAA coral reef watch program's near-real time satellite global coral bleaching monitoring activities. In Proceedings of the 10th international coral reef symposium (Vol. 1793, pp. 1783-1793). Gurugram: Okinawa.

Loya, Y. (1972). Community structure and species diversity of hermatypic corals at Eilat, Red Sea. Marine Biology, 13, 100-123.

Lyakhovsky, V., Segev, A., Schattner, U., & Weinberger, R. (2012). Deformation and seismicity associated with continental rift zones propagating toward continental margins. Geochemistry, Geophysics, Geosystems, 13(1).

Madah, F., Mayerle, R., Bruss, G., & Bento, J. (2015). Characteristics of tides in the Red Sea region, a numerical model study. Open journal of marine science, 5(02), 193.

Mason, R. A., Skirving, W. J., & Dove, S. G. (2020). Integrating physiology with remote sensing to advance the prediction of coral bleaching events. *Remote Sensing of Environment*, *246*, 111794.

McKenzie, D. P., Davies, D., & Molnar, P. (1970). Plate tectonics of the Red Sea and east Africa. Nature, 226(5242), 243-248.

McPhaden, M. J., & Yu, X. (1999). Equatorial waves and the 1997–98 El Niño. Geophysical Research Letters, 26(19), 2961-2964.

Mona, M. H., El-Naggar, H. A., El-Gayar, E. E., Masood, M. F., & Mohamed, E. S. N. (2019). Effect of human activities on biodiversity in nabq protected area, south sinai, Egypt. *The Egyptian Journal of Aquatic Research*, *45*(1), 33-43.

Mora, C., & Sale, P. F. (2011). Ongoing global biodiversity loss and the need to move beyond protected areas: a review of the technical and practical shortcomings of protected areas on land and sea. Marine ecology progress series, 434, 251-266.

Morcos, S. A. (1970). Physical and chemical oceanography of the Red Sea. Oceanogr. Mar. Biol. Annu. Rev, 8(73), 202.

Morgan, P., Aplet, G. H., Haufler, J. B., Humphries, H. C., Moore, M. M., & Wilson, W. D. (1994). Historical range of variability: a useful tool for evaluating ecosystem change. Journal of Sustainable forestry, 2(1-2), 87-111.

Muller-Parker, G., D'elia, C. F., & Cook, C. B. (2015). Interactions between corals and their symbiotic algae. In *Coral reefs in the Anthropocene* (pp. 99-116). Springer, Dordrecht.

Muscatine, L. (1990). The role of symbiotic algae in carbon and energy flux in reef corals. Coral reefs, 25(1.29), 75-87.

Nandkeolyar, N., Raman, M., & Kiran, G. S. (2013). Comparative analysis of sea surface temperature pattern in the eastern and western gulfs of Arabian Sea and the Red Sea in recent past using satellite data. International Journal of Oceanography, 2013.

Ormond, R. F. G., & Edwards, A. J. (1987). Red Sea fishes. Red Sea, 7, 251.

Pandolfi, J. M., & Jackson, J. B. (2006). Ecological persistence interrupted in Caribbean coral reefs. Ecology Letters, 9(7), 818-826.

Pandolfi, J. M., Bradbury, R. H., Sala, E., Hughes, T. P., Bjorndal, K. A., Cooke, R. G., ... & Jackson, J. B. (2003). Global trajectories of the long-term decline of coral reef ecosystems. Science, 301(5635), 955-958.

Patzert, W. C. (1974, February). Wind-induced reversal in Red Sea circulation. In Deep Sea Research and Oceanographic Abstracts (Vol. 21, No. 2, pp. 109-121). Elsevier.

Pauly, D., & Froese, R. (2012). Comments on FAO's State of Fisheries and Aquaculture, or 'SOFIA 2010'. Marine Policy, 36(3), 746-752.

Plaisance, L., Caley, M. J., Brainard, R. E., & Knowlton, N. (2011). The diversity of coral reefs: what are we missing? PloS one, 6(10), e25026.

Phillips, J. D. (1970). A discussion on the structure and evolution of the Red Sea and the nature of the Red Sea, Gulf of Aden and Ethiopia rift junction-Magnetic anomalies in the Red Sea. Philosophical Transactions of the Royal Society of London. Series A, Mathematical and Physical Sciences, 267(1181), 205-217.

Polovina, J. J. (1984). Model of a coral reef ecosystem. Coral reefs, 3(1), 1-11.

Purkis, S. J., Gleason, A. C., Purkis, C. R., Dempsey, A. C., Renaud, P. G., Faisal, M., ... & Kerr, J. M. (2019). High-resolution habitat and bathymetry maps for 65,000 sq. km of Earth's remotest coral reefs. Coral Reefs, 38(3), 467-488.

Raitsos, D. E., Pradhan, Y., Brewin, R. J., Stenchikov, G., & Hoteit, I. (2013). Remote sensing the phytoplankton seasonal succession of the Red Sea. PloS one, 8(6), e64909.

Raitsos, D. E., Yi, X., Platt, T., Racault, M. F., Brewin, R. J., Pradhan, Y., ... & Hoteit, I. (2015). Monsoon oscillations regulate fertility of the Red Sea. Geophysical Research Letters, 42(3), 855-862.

Ramesh, C. H., Koushik, S., Shunmugaraj, T., & Murthy, M. V. R. (2020). Seasonal studies on in situ coral transplantation in the Gulf of Mannar Marine Biosphere Reserve, Southeast coast of Tamil Nadu, India. Ecological Engineering, 152, 105884.

Rao, N. D., & Behairy, A. K. A. (1986). Nature and composition of shore-zone sediments between Jeddah and Yanbu, eastern Red Sea. Marine geology, 70(3-4), 287-305.

Rasul, N. M., Stewart, I. C., & Nawab, Z. A. (2015). Introduction to the Red Sea: its origin, structure, and environment. In *The Red Sea: The formation, morphology, oceanography and environment of a young ocean basin* (pp. 1-28). Berlin, Heidelberg: Springer Berlin Heidelberg.

Reaser, J. K., Pomerance, R., & Thomas, P. O. (2000). Coral bleaching and global climate change: scientific findings and policy recommendations. Conservation biology, 14(5), 1500-1511.

Riegl, B. M., Bruckner, A. W., Rowlands, G. P., Purkis, S. J., & Renaud, P. (2012). Red Sea coral reef trajectories over 2 decades suggest increasing community homogenization and decline in coral size. PLoS One, 7(5), e38396.

Schgal, R. (2006). Legal Regime Towards Protecting Coral Reefs: An International Perspective and Indian Scenario. Law Env't & Dev. J., 2, 183.

Scoffin, T. P. (1993). The geological effects of hurricanes on coral reefs and the interpretation of storm deposits. Coral Reefs, 12(3), 203-221.

Searle, R. C., & Ross, D. A. (1975). A geophysical study of the Red Sea axial trough between 20· 5° and 22° N. Geophysical Journal International, 43(2), 555-572.

Sebhatu, T.G. (2019, December). 6th National Report to the Convention on Biological Diversity-Eritrea.

Selig, E. R., Casey, K. S., & Bruno, J. F. (2010). New insights into global patterns of ocean temperature anomalies: implications for coral reef health and management. Global Ecology and Biogeography, 19(3), 397-411.

Smith, J. E., Brainard, R., Carter, A., Grillo, S., Edwards, C., Harris, J., ... & Sandin, S. (2016). Re-evaluating the health of coral reef communities: baselines and evidence for human impacts across the central Pacific. Proceedings of the Royal Society B: Biological Sciences, 283(1822), 20151985.

Sofianos, S. S., & Johns, W. E. (2007). Observations of the summer Red Sea circulation. Journal of Geophysical Research: Oceans, 112(C6).

Solanki, H. U., Mankodi, P. C., Nayak, S. R., & Somvanshi, V. S. (2005). Evaluation of remote-sensing-based potential fishing zones (PFZs) forecast methodology. Continental shelf research, 25(18), 2163-2173.

Solayan, A. (2016). Biomonitoring of coral bleaching—A glimpse on biomarkers for the early detection of oxidative damages in corals (pp. 101-117). InTech.

Spalding, M. D., & Brown, B. E. (2015). Warm-water coral reefs and climate change. Science, 350(6262), 769-771.

Steckler, M. S., & ten Brink, U. (1986). Lithospheric strength variations as a control on new plate boundaries: Examples from the northern Red Sea region: Earth and Planetary Letters, v. 79. doi, 10, 90045-2.

Tesfamichael, D. (2016). An Exploration of Ecosystem-Based Approaches for the Management of Red Sea Fisheries. In The Red Sea Ecosystem and Fisheries (pp. 111-134). Springer, Dordrecht.

Tsehaye, I., Machiels, M. A., & Nagelkerke, L. A. (2007). Rapid shifts in catch composition in the artisanal Red Sea reef fisheries of Eritrea. Fisheries research, 86(1), 58-68.

Van de Leemput, I. A., Hughes, T. P., van Nes, E. H., & Scheffer, M. (2016). Multiple feedbacks and the prevalence of alternate stable states on coral reefs. Coral Reefs, 35(3), 857-865.

Van Duyl, F., Gast, G., Steinhoff, W., Kloff, S., Veldhuis, M., & Bak, R. (2002). Factors influencing the short-term variation in phytoplankton composition and biomass in coral reef waters. Coral Reefs, 21, 293-306.

Veron, J. E. N. (2002). New species described in Corals of the World (Vol. 11). Townsville: Australian Institute of Marine Science.

Vine, P. (2019). Red Sea Research: A Personal Perspective. In Oceanographic and Biological Aspects of the Red Sea (pp. 215-237). Springer, Cham.

Whitmarsh, G. (1974). The politics of political education: an episode. Journal of Curriculum Studies, 6(2), 133-142.

Wilkinson, C. R. (1999). Global and local threats to coral reef functioning and existence: review and predictions. Marine and freshwater research, 50(8), 867-878.

Wilkinson, C. (2000). Status of coral reefs of the world: 2000. Australian Institute of Marine Science.

Wilkinson, C. R., & Souter, D. (2008). Status of Caribbean coral reefs after bleaching and hurricanes in 2005.

Williams, G. J., Gove, J. M., Eynaud, Y., Zgliczynski, B. J., & Sandin, S. A. (2015). Local human impacts decouple natural biophysical relationships on Pacific coral reefs. Ecography, 38(8), 751-761.

Wolanski, E., Richmond, R., McCook, L., & Sweatman, H. (2003). Mud, marine snow and coral reefs: the survival of coral reefs requires integrated watershed-based management activities and marine conservation. American Scientist, 91(1), 44-51.

Yao, F., Hoteit, I., Pratt, L. J., Bower, A. S., Zhai, P., Köhl, A., & Gopalakrishnan, G. (2014). Seasonal overturning circulation in the Red Sea: 1. Model validation and summer circulation. Journal of Geophysical Research: Oceans, 119(4), 2238-2262.

Zekeria, Z. A. (2003). Butterflyfishes of the southern Red Sea: ecology and population dynamics.